A Voting-Based Femtocell Downlink Cell-Breathing Control Mechanism

Chih-Yu Wang, Chun-Han Ko, Hung-Yu Wei, and Athanasios V. Vasilakos, *Senior Member, IEEE*

***Abstract*—An overlay macrocell-femtocell system aims to increase the system capacity with a low-cost infrastructure. To construct such an infrastructure, we need to solve some existing problems. First, there is a tradeoff between femtocell coverage and overall system throughput, which we defined as the cell-breathing phenomenon. In light of this, we propose a femtocell downlink cell-breathing control framework to strike a balance between the coverage and data rate. Second, due to the selfish nature of mobile stations, the system information collected from them does not necessarily reflect the true status of the system. Thus, we design FEmtocell Virtual Election Rule (FEVER), a voting-based direct mechanism that only requires users to report their channel quality information to the femtocell base station. Not only is it proved to be truthful and has low implementation complexity, but it also strikes a balance between efficiency and fairness to meet the different needs. The simulation results verify the enhanced system performance under the FEVER mechanism.**

***Index Terms*—Game theory, overlay network, voting theory.**

I. Introduction

AN OVERLAY macrocell-femtocell system aims to enhance the system capacity in a low-cost and self-organized manner [1]. A femtocell base station (BS) with low transmission power can be installed in indoor or natural environments to overcome a macrocell's severe signal degradations. Since the mobile stations (MSs) in these environments are at relatively shorter distances from the femtocell than the macrocell, their signal qualities are enhanced with the lower radio propagation loss. Thus, the cellular system capacity is enhanced by the femtocell. In practical implementation, femtocell BSs are usually deployed by users themselves in an unplanned manner and operate through existing personal broadband connections. These connections with limited data rates will be used as backhaul links of femtocells. Hence, the femtocell system should be self-organized in order to prevent unnecessary interference and resource wastes [2].

Manuscript received January 07, 2011; revised January 25, 2012; January 25, 2012; and February 17, 2014; accepted September 06, 2014; approved by IEEE/ACM TRANSACTIONS ON NETWORKING Editor L. Ying. Date of publication October 03, 2014; date of current version February 12, 2016. The work of H.-Y. Wei was supported by the Ministry of Science and Technology under Grants 103-2221-E-002-086-MY3 and 102-2221-E-002-077-MY2. *(Corresponding author: Hung-Yu Wei.)*

C.-Y. Wang and C.-H. Ko are with the Graduate Institute of Communication Engineering, National Taiwan University, Taipei, Taiwan (e-mail: tomkywang@gmail.com; d01942010@ntu.edu.tw).

H.-Y. Wei is with the Graduate Institute of Communication Engineering and Department of Electrical Engineering, National Taiwan University, Taipei, Taiwan (e-mail: hywei@cc.ee.ntu.edu.tw).

A. V. Vasilakos is with Kuwait University, Safat 13060, Kuwait (e-mail: vasilako@ath.forthnet.gr).

Color versions of one or more of the figures in this paper are available online at http://ieeexplore.ieee.org.

Digital Object Identifier 10.1109/TNET.2014.2357498

A. Femtocell Coverage Control and Cell-Breathing

The coverage of the femtocell should be properly chosen according to the demand from user equipments (UEs) and expected loading in the overlay system. The coverage of the femtocell is mostly determined by the transmission power of the femtocell BS. An increase in the transmission power generally leads to enhancement in signal quality to all UEs, and an increase in coverage since some near-edge UEs now have an acceptable signal quality from the femtocell. Nevertheless, a larger coverage usually means more UEs served by the femtocell, which could be a source of congestion when the femtocell is limited in the wireless resource or backhaul capacity. In fact, we observe that there is a tradeoff between system throughput and coverage in downlink scheme of an overlay macrocell-femtocell system, which we denoted as the cell-breathing phenomenon. The coverage of the femtocell should be carefully chosen according to the loading of the overlay system in order to prevent unnecessary waste or congestion, as we will illustrate in the following example.

We examine an overlay system with one macrocell and one femtocell as an example. MSs located in the overlay section of both cells can freely choose the serving cell from these two cells. In general, MSs' choices on the cells mainly depend on the offered service quality. Based on the system efficiency perspective, only a limited number of MSs with good channel qualities are supposed to be served by the femtocell. Other MSs should be served by the macrocell in order to preserve the limited femtocell resources.

The limitations on the femtocell resources come from two parts: wired backhaul data rate and wireless resources. The wired backhaul data rate becomes the limitation when femtocells operate through existing broadband connections with limited data rate compared to the macrocells deployed by the service operators. The wireless resources become the limitation when femtocells are only allowed to use limited wireless resources such as spectrum or access time since they usually operate in a lower coverage and loading on average compared to the macrocells. Note that both limitations can be considered as the constraints on the capacity of the femtocells.

The cell-breathing phenomenon in an overlay macrocell-femtocell system arises when the femtocell backhaul data rate becomes the stricter constraint of the femtocell throughput. When the backhaul data rate is the stricter constraints, those MSs served by the femtocell may experience a low throughput. It happens when the coverage of the femtocell is not properly configured. We illustrate an example in Fig. 1, where an overlay macrocell-femtocell system is serving five MSs. The femtocell

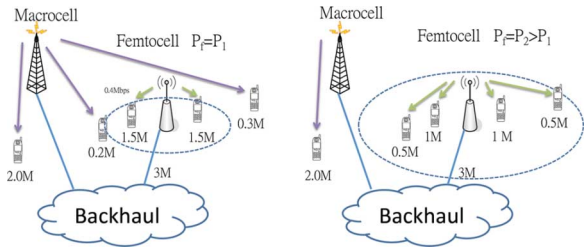

Fig. 1. Downlink cell-breathing in an overlay macrocell-femtocell system.

BS has a 3-Mb/s backhaul connection. When the femtocell BS's downlink transmission power is P_1, it provides a small coverage and therefore only serves two MSs. Each of the MSs has a throughput of 1.5 Mb/s. The total backhaul data rate, which is 3 Mb/s, has been allocated to these two MSs. For other MSs, they are served by the macrocells. The overall achieved system throughput under P_1 is 5.4 Mb/s. Then, when the femtocell BS increases its downlink power from P_1 to $P_2(P_2 > P_1)$, the coverage of the femtocell increases. Four, instead of two, MSs can be served by the femtocell. The newly joined MSs will choose the femtocell as their serving cell since the femtocell provides a higher expected throughput (0.5 Mb/s) to them. Nevertheless, the original two MSs experience a lower throughput compared to the data rate under P_1, which is because the overall femtocell throughput is constrained by the limited backhaul data rate. In such a case, the overall achieved system throughput is reduced to 3 Mb/s + 2 Mb/s = 5 Mb/s. The efficiency loss is due to the unbalanced loading between the macrocell and femtocell. The increased femtocell coverage benefits some MSs originally served by the macrocell, but degrades the data rates of other MSs who are already served by the femtocell. The backhaul resource utilization turns out to be inefficient when too many MSs choose to be served by the femtocell. In short, *increasing femtocell downlink transmission power may result in the degradation of MSs' downlink throughput and impair the utilitarian of the overall system resource*.

1) Self-Organized Femtocells With Rational MSs: Because of the femtocell's unplanned deployment characteristic, traditional optimization techniques cannot be applied before installations. Thus, the femtocell system should be designed as a self-organized system. When the femtocell BS tries to organize and decide proper system parameters, such as downlink transmission power, comprehensive information on the overlay system, including the backhaul data rate, downlink channel quality information (CQI) of MSs, throughput and delay constraints of the traffic, etc., is required. The femtocell BS relies on the reports from the MSs to collect the information. For instance, the femtocell BS requests a CQI report from the MS to derive the CQI of MSs. However, since the choice of the system parameter, such as coverage, is related to the information reported by MSs, this creates an issue in the self-organized femtocell: cheating behavior of MSs.

MSs are distributed devices controlled by users, who are rational beings and behave selfishly. Their behavior is based on their own benefits, which may be conflicted with the system optimization objective. In the femtocell system we discussed in the previous paragraph, there is a chance that MSs may report unauthentic information that does not reflect the true system state but can persuade the femtocell to make the action that enhances the cheating MSs' benefits.

Let us consider several traditional access policies and see how selfish MSs may choose to report fake information here.

1) The femtocell chooses to serve k MSs with worst channel qualities in macrocell. The femtocell downlink transmission power will then be adjusted to allow those users to be served by the femtocell. When an MS is rational, it has the incentive to report a lower channel quality in CQI report since it then has a higher probability to be served by the femtocell.
2) The femtocell chooses to serve k MSs with highest channel qualities in femtocell. In this case, MSs tend to report higher channel quality in CQI reports in order to increase the probability to be served by the femtocell. Specifically, a selfish MS tends to report an untruthful signal-to-noise ratio (SNR) in the CQI report, which is a higher SNR that leads to the same modulation and coding scheme (MCS) as the one if the true signal-to-interference-plus-noise ratio (SINR) is reported. According to the MCS-SINR table for IEEE 802.16m [3] and 3 GPP LTE [4] suggested in the literature, we observe that a typical MCS SINR range is $1 \sim 3$ dB wide. This suggests that there is always room for cheating: An MS may report a 3-dB higher SINR to the BS without altering the selected MCS. By reporting a higher SINR, the probability to be served by the femtocell increases. Within an MCS SINR range, the difference in throughput is $0.2 \sim 0.5$ Mb/s. This gap is the damage a cheating MS may cause to the system. When N MSs cheat by reporting higher SINR, these MSs may occupy the femtocell, kick out other MSs with better SINR, and therefore decrease overall system throughput up to $0.5 \times N$ Mb/s.
3) The femtocell chooses to serve k most delay-sensitive MSs for data services. Local IP access (LIPA) is one of the planning features in LTE to offload the traffic from the core networks. Through LIPA, some data traffic such as Web browsing will go through the broadband connection to the Internet directly without the unnecessary rerouting to the core network. It is ideal for LIPA-enabled femtocells to allow MSs who request delay-sensitive services to access. Nevertheless, MSs may have the incentive to report themselves as delay-sensitive ones with a strict delay constraint regardless of their true QoS requirement since a shorter delay is always welcomed. Through reporting a strict delay constraint, the probability that the cheating MS is allowed to access the femtocell and utilize LIPA increases.

In the above examples, we observe that rational MSs are likely to be cheated under traditional access policy by reporting fake information. When the collected information does not reflect the true system status, *the decision of the femtocell will deviate from the optimization choice due to the selfish behavior of MSs*, which is not a desired situation from the system optimization perspective. Such cheating behaviors can be considered as a source to the instability of the overlay system, which should be prevented by truth-telling designs in advance in order to maintain the robustness of the system.

2) Subscriber Group Modes: Subscriber group mode is another important feature in the self-organized femtocell system. A subscriber group can be optionally defined in the femtocell for access control. Three subscriber group modes are defined in the femtocell system: Open Subscriber Group (OSG), Closed Subscriber Group (CSG), and Hybrid mode [5]. In OSG mode, all users are allowed to access the femtocell service. In contrast, a femtocell in CSG mode only allows access to users in the subscriber group. As a balanced design between OSG and CSG, in Hybrid-mode subscriber group, users can access the femtocell service at any time, while nonsubscriber group users can access it under a lower priority. Although Hybrid mode offers a flexible resource allocation approach, the selfish behavior of MSs becomes a more serious issue under Hybrid mode because of different types of MSs. Different types of MSs may compete with each other by persuading the femtocell favoring one of the groups and blocking the other.

In this work, we analyze the cell-breathing phenomenon resulting from the femtocell downlink power control through the proposed femtocell cell-breathing control framework. Due to the selfish behavior of MSs in a wireless network, we need a truthful information collecting mechanism to ensure the authenticity of the reported QoS information, such as CQI and delay constraints, from MSs. We therefore propose a *voting-based FEmtocell Virtual Election Rule* (FEVER) mechanism. Voting has been popularly used in our daily life and well studied to determine policies related to mass publics [6]. We observe that the voting process highly matches our cell-breathing control framework—the femtocell's transmission power should be determined by the information (opinions) provided by the MSs. We prove that in the FEVER mechanism, all MSs truthfully report their quality-of-service (QoS) information without the incentive to manipulate. Additionally, the FEVER mechanism provides the flexibility to satisfy different requirements in the balance between efficiency and fairness. For those three subscriber group modes, we propose the Subscriber Group FEVER (SG-FEVER) mechanism to: 1) guarantee the service quality of subscriber group users; and 2) maintain the truthfulness and flexibility of the FEVER mechanism.

Additionally, unlike other popular truthful mechanisms one may find in spectrum auction [7] or cloud computing [8], requiring a monetary transfer process to properly function, the FEVER mechanism only requires the QoS information reporting (vote) from voters. This reduces the complexity of the mechanism and makes it easily implemented to the existing wireless system with existing feedback processes.

The main contributions of this paper are listed as follows.

1) The cell-breathing phenomenon in an overlay macrocell-femtocell system is described and investigated. We propose a novel femtocell cell-breathing control framework for managing the load balancing and coverage control among overlay cells.
2) We formulate a game-theoretical model for discussing the cheating issue in an overlay network with selfish mobile stations. We introduce the concept of voting theory into the cell-breathing control framework. The proposed voting-based FEVER mechanism is proved to be truthful. It also offers the flexibility to strike a balance between capacity efficiency and allocation fairness in the proposed framework.
3) For evaluating the system performance, an LTE overlay network simulator is implemented with realistic radio propagation and modulation models [9], [10]. The efficiency and fairness under different parameter settings in the FEVER mechanism are verified through simulations. We further investigate and compare the three subscriber group modes under the SG-FEVER mechanism to the LTE simulator. The characteristics of these three modes are demonstrated in realistic simulations.

B. Related Work

Veeravalli and Sendonaris first discovered the cell-breathing phenomenon in a CDMA cellular system [11]. Jalali further discussed the possibility of using cell-breathing phenomenon as a management tool on the cell capacity [12]. The fairness issue under cell-breathing was investigated by Yang and Ephremides [13]. Besides a CDMA system, researchers also observed the cell-breathing phenomenon in the coverage of WLAN AP [14], [15]. Bahl *et al.* proposed various cell-breathing control algorithms under WLAN to realize power estimation and load balancing [14]. Bejerano and Han also proposed graph-based cell-breathing algorithms to realize the load balancing [15].

For research on the femtocell subscriber group modes [5], studies have showed that either static CSG or OSG modes may result in system inefficiency in interference management and bandwidth sharing [16]–[19]. Hybrid mode as a balance between interference and efficiency was suggested in [18] and [19]. The implementation of Hybrid mode in an OFDMA system was further discussed in [20].

Some related works have focused on the issue of downlink power control in femtocell networks. Akbudak and Czylwik designed a distributed power control and scheduling algorithm to mitigate co-tier interference between femtocells. Through numerical analysis, they showed that their designed algorithm achieved suboptimum close to global optimum [21]. Li *et al.* proposed both centralized and distributed solutions to reduce cross-tier interference in macrocell-femtocell overlay networks. The proposed solutions provide QoS to both macrocell and femtocell users [22]. Jorswieck and Mochaourab used game theory to analyze the noncooperative power allocation between two cells in cellular networks. In addition, they applied an AGV mechanism to guarantee MSs' truthful SINR reporting [23]. However, these works focus on the wireless capacity of the multicell system, while the backhaul capacity constraint in a femtocell is not in their scopes.

To the best of our knowledge, the issue of cell-breathing downlink power control in backhaul-constrained overlay networks has not been covered yet.

II. Femtocell Cell-Breathing Framework

We start from an overlay macrocell-femtocell system. A macrocell BS serves MSs in its coverage area. One femtocell BS is located in the macrocell's coverage area, with one coverage area overlapping with the former one. Both BSs are operating with backhaul connections with certain data rates. For analysis simplification, the macrocell and femtocell use different spectrums in our model, so there is no intercell interference issue in the overlay system. Note that the main

TABLE I
NOTATIONS

Notation	Explanation
S, S_f, S_m	The set of MSs (all, in femtocell, in macrocell)
$L_{i,\{f,m\}}$	The channel quality information (CQI) of M_i
P_f	The femtocell downlink power
$\eta_{i,\{f,m\}}$	The SINR experienced by M_i
$\Gamma(\eta_i)$	The wireless data rate of M_i under SINR η_i
$\Gamma_{i,f}(P_f)$	The wireless data rate of M_i from the femtocell under P_f
$A(\cdot)$	The femtocell's allocation rule on downlink data rate
$\gamma_{i,\{f,m\}}$	The expected throughput of M_i
$B(\cdot)$	The downlink cell-breathing rule

conclusion of this paper is not affected even if the cells share the same spectrum, which is discussed in Section IV.

We are focusing on the downlink wireless transmission of MSs in this paper. There are N MSs $M_i \in S$ in the coverage of femtocell. An MS can be served by either the macrocell or femtocell. We denote the set of MSs served by the macrocell and the femtocell by S_{m} and S_{f}, respectively. The notations are summarized in Table I. For a given cell $j = \{\mathrm{f}, \mathrm{m}\}$, the BS transmits downlink data to MSs by a power P_j in a carrier. For an MS M_i served by the cell j, its downlink SINR is $\eta_{i,j} = \frac{P_j G_{i,j}}{N_0 + I_{i,j}}$ where $G_{i,j}$ is the signal-loss rate from cell j to M_i, N_0 is the background white noise, and $I_{i,j}$ is the location-dependent interference. We use $L_{i,j} = \frac{G_{i,j}}{N_0+I_{i,j}}|_{j=\{\mathrm{m},\mathrm{f}\}} \in \Lambda$ to denote the CQI of M_i in cell j, where Λ is the universal set of CQI. For a given SINR $\eta_{i,j}$, we denote the wireless data rate from cell j to M_i by $\Gamma(\eta_{i,j})$, which is the PHY transmission rate in a typical wireless communication system. We assume $\Gamma(\cdot)$ is an increasing function, which is true in most modulation schemes.

A. Cell-Breathing Phenomenon

Given the same network scenario (macrocell BS's downlink power, all MSs' signal loss rates, etc.), when the femtocell BS increases its downlink power P_{f}, we observe that there are two opposite influences on the MSs. On one hand, it enhances the wireless transmission qualities of MSs served by the femtocell. To be specific, an MS M_i's SINR $\eta_{i,\mathrm{f}} = P_{\mathrm{f}} L_{i,\mathrm{f}}$ increases linearly with P_{f}, and its wireless data rate $\Gamma(\eta_{i,\mathrm{f}})$ increases with P_{f} because $\Gamma(\eta_{i,\mathrm{f}})$ is an increasing function (for convenience, we denote $\Gamma(P_{\mathrm{f}} L_{i,\mathrm{f}})$ by $\Gamma_{i,\mathrm{f}}(P_{\mathrm{f}})$). On the other hand, because the downlink transmission in the femtocell is enhanced, some MSs may choose to select the femtocell instead of macrocell as their serving cell. Thus, MSs already served by the femtocell may have a lower expected throughput due to the joining of new MSs. The *cell-breathing phenomenon* is composed of these two effects. Note that this is different from the cell-breathing in a CDMA system [11]. In the case of CDMA cell-breathing, an increase in the cell coverage results in a decrease in the cell's capacity due to interference among MSs in the same cell. In contrast, in an OFDMA system, the overall throughput in general increases with the transmission power until it is constrained by the wired backhaul data rate. However, the overlay system throughput may decrease when the femtocell's coverage increases since MSs may inefficiently choose the femtocell as their serving cell and therefore reduce the overall resource utilization.

Additionally, the coverage of a femtocell should be self-organized according to the current cell deployment and resource availability of the overlay system. In traditional cellular networks, the cell coverage is usually properly planned by a telecom operator in advance. On the contrary, femtocell base stations are typically deployed in an unplanned manner [1], [2]. In this paper, we assume that the femtocell has been deployed by the user, and therefore the cell deployment is given in advance. In such a scenario, we consider the self-organized femtocell coverage control problem given that the femtocell base stations are already deployed. The optimal cell planning, which is another interesting issue, is beyond the scope of this paper.

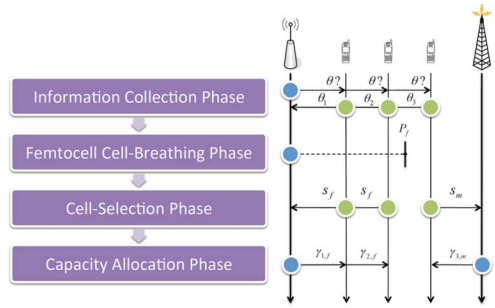

Fig. 2. Femtocell cell-breathing control framework.

Due to the cell-breathing phenomenon, a proper choice on the P_{f} is important for femtocells to enhance the downlink transmission qualities of MSs while serving a reasonable number of MSs. This requires CQI reported by MSs. Thus, we propose a cell-breathing control framework, which has four phases: *Information Collection, Femtocell Cell-breathing, Cell Selection,* and *Capacity Allocation phases* (Fig. 2).

B. Information and Cell-Breathing Control Phases

In the Information Collection phase, the femtocell defines the information it requires, which we denoted as θ here. All MSs in the area report their information θ_i to the femtocell then. Notice that we do not specify the type of information here since it depends on the application. The information can be CQI, delay constraint, or other QoS-related information. Next, in Femtocell Cell-Breathing phase, the femtocell decides P_{f} in accordance with the $\{\theta_i\}$ collected in the first phase. We denote a downlink cell-breathing rule B based on the collected $\bar{\theta} = \{\theta_i\} \in \Theta^n$ by a function B

$$B : \Theta^n \mapsto [0, P_{\mathrm{f}}^{\max}] \Rightarrow B(\bar{\theta}) = B(\{\theta_i\}) = P_{\mathrm{f}}$$

where θ_i is the information reported by M_i, Θ^n is the universal set of information, and $P_{\mathrm{f}}^{\max}$ is the maximum power.

Since the information is only known by the MSs themselves and unknown to the femtocell BS, MSs may "cheat" by reporting false information to mislead the femtocell's choice on P_{f}. Cheating not only leads to unfairness in the system, but also makes the femtocell choose an improper P_{f} and degrades the system performance. To prevent cheating, the downlink cell-breathing rule should be truthful, that is, after all selfish MSs learned the rule, they all choose to report the true information.

In this framework, the information is reported by MSs in the first phase, and then the femtocell BS chooses the downlink transmission power in second phase. If the information required is MSs' preferred downlink power, these two phases naturally

formulate a *voting scheme* , and the cell-breathing rule can be considered as a *voting rule*.

Voting is an important research topic in economics and politics. The main concept of voting is aggregating voter's votes on several public policies. Then, a predefined voting rule chooses one vote as the output. The most commonly used voting rule is the majority rule, which chooses the policy that most voters vote for. Unfortunately, the majority rule has been proved to be untruthful and easy to be manipulated. Thus, it is not applicable in this framework. *Median Voter Scheme* (MVS) is a popular truthful voting design. It is used to choose a public policy $r \in R$ that can be one-to-one transformed into a real value set $\bar{R} \subset [0,1]$. The procedure of MVS is as follows.

1) The election holder announces what order of the sorted votes he will choose (the median one, for instance).
2) All voters vote for their preferred policy v_i.
3) The election holder chooses the votes according to the rule he claimed before as the output of the election.

Mathematically, given a sorted vote set $V = \{v | v_i \leq v_j \forall i < j\}$ in ascending order and a predetermined selected vote order κ, the output of MVS is v_κ. Based on MVS, we propose the *Virtual Election Scheme* for cell-breathing control in this framework. Given all MSs $M_i \in S$'s vote p_i on the femtocell downlink power P_{f} and a predefined selected vote order κ, we denote the Virtual Election rule as

$$B_v(\bar{p}, \kappa) = B_v(\{p | p_i \leq v_j \forall i, j \leq N, i < j\}, \kappa) = p_\kappa. \quad (1)$$

C. Cell Selection and Capacity Allocation Phases

The expected throughput, which is the main concern of the MSs and is denoted by γ, is then determined in Cell Selection and Capacity Allocation phases. After the femtocell BS chooses the downlink power in the Cell-Breathing Phase, MSs select the cell to be served in the Cell Selection phase. The MS's selection on the cell is based on the expected throughput under different cells, which will be determined in the Capacity Allocation phase, where femtocell and macrocell BSs allocate their backhaul capacity to the MSs they serve. The expected throughput of an MS is under the constraints of both wireless data rate and allocated backhaul data rate. Therefore, an MS should carefully choose the cell by considering both data rates in each cell.

In this framework, we assume the backhaul data rate of macrocell BS is large enough to handle all serving MSs' downlink request since it is deployed directly through the service provider. Mathematically, its backhaul data rate, which is denoted as C_{m}, is larger than the sum of serving MSs' wireless data rate $\sum_{M_i \in S_{\mathrm{m}}} \Gamma(\eta_{i,\mathrm{m}})$. Hence, for M_i requiring the data from the Internet, its expected throughput, which is denoted by $\gamma_{i,\mathrm{m}}$, is always exactly its wireless data rate, that is, $\gamma_{i,\mathrm{m}} = \Gamma(\eta_{i,\mathrm{m}})$.

However, in the case of the femtocell BS, the allocation of available backhaul capacity becomes an issue. The data rate C_{f} of a femtocell backhaul connection is usually limited because it is installed at home or the office and using a broadband connection as its backhaul. It is possible that available resources cannot meet the total wireless data rate of all serving MSs, that is, $C_{\mathrm{f}} < \sum_{M_i \in S_{\mathrm{f}}} \Gamma(\eta_{i,\mathrm{f}})$. Thus, the allocated downlink data rate of M_i under femtocell, which is denoted by $\gamma_{i,\mathrm{f}}$, is less than or equal to $\Gamma(\eta_{i,\mathrm{f}})$. Under this circumstance, not all MSs can have downlink transmission at their maximum achievable data rate. Thus, a predefined allocation rule is required. We denote an allocation rule to allocate C_{f} to all MSs served by the femtocell by

$$A(\{\Gamma(\eta_{i,\mathrm{f}}) | M_i \in S_{\mathrm{f}}\}) = \{\gamma_{i,\mathrm{f}} | M_i \in S_{\mathrm{f}}\}. \quad (2)$$

Each MS is allocated with a backhaul data rate $\gamma_{i,j}|_{j=\{\mathrm{m},\mathrm{f}\}}$ according to their wireless data rate and the total backhaul data rate. A reasonable backhaul data rate allocated to an MS should not exceed its wireless data rate. Therefore, the allocated backhaul data rate is also its expected throughput under the cell. For a femtocell BS, the allocation rule $A(\cdot)$ is applied to determine all MSs' expected throughput $\gamma_{i,\mathrm{f}}$. Since fairness is typically a desirable property in the resource allocation problem, we consider a fair allocation rule $A(\cdot)$ in this framework. We define the fairness of the allocation rule $A(\cdot)$ as follows.

Assumption 1 (Max-Min Fairness): For an allocation rule $A(\{\Gamma(\eta_{i,\mathrm{f}}) | M_i \in S_{\mathrm{f}}\}) = \{\gamma_{i,\mathrm{f}} | M_i \in S_{\mathrm{f}}\} = \gamma^{\mathrm{f}}, \forall M_i,\ M_j \in S_{\mathrm{f}}$, the following assumptions must be satisfied:

$$\begin{aligned} &\text{if } \exists \gamma'^{f} \neq \gamma^{\mathrm{f}}, \gamma'_{k,\mathrm{f}} > \gamma_{k,\mathrm{f}} \text{ for some } M_k \in S_{\mathrm{f}} \\ &\quad \Rightarrow \exists M_i \in S_{\mathrm{f}}, \gamma'_{i,\mathrm{f}} < \gamma_{i,\mathrm{f}} \leq \gamma_{k,\mathrm{f}}. \end{aligned} \quad (3)$$

A straightforward thinking of this assumption is some backhaul capacity originally allocated to the existing MSs served by the femtocell may be reallocated to the new MS in order to ensure fairness. In fact, (3) is a general characteristic for an allocation rule with max-min fairness constraints [24].

In addition, we assume $\forall M_i \in S$, $\frac{C_{\mathrm{f}}}{N} \geq \gamma_{i,\mathrm{m}}$, which we call the capacity assumption. This catches the characteristics of femtocell deployment in the real world: Femtocells mostly are installed in the environments where the macrocell cannot offer good service qualities. In addition, a service provider may support a user to install a femtocell BS by upgrading the user's broadband connection in order to make the femtocell capable of accommodating multiple MSs. In Section V-B, we show that the assumption can be relaxed when our objective is maximizing overall system throughput.

III. Game Model Formulation and Analysis

We now characterize MSs' behavior in the proposed framework. Generally, a rational MS should select the BS that offers the higher expected throughput as its serving BS. Notice that the expected throughput depends on two factors. The first factor is the wireless data rate of the serving MS, which is affected by the downlink transmission power of the BS. The second factor is the allocated backhaul data rate, which is determined by the amount of the backhaul resource that the BS will allocate to the MS. Specifically, the data rate the BS allocated to an MS depends on the channel quality under the cell and the number of MSs served by the cell. Since the expected throughput under a cell will be influenced by the choice of other MSs, an MS's optimal choice will be determined by other MSs' decisions in the Cell Selection phase.

These complicated interactions should be investigated in order to ensure the final operating point is the one we desire. Game Theory is an appropriate tool in formulating and analyzing such a system. We use the Nash Game model to formulate the cell-breathing control problem. Nash Equilibrium of the cell-breathing control problem, which represents the stable operating point in the system, is analyzed.

In a Nash Game model, there are three components: *players*, *actions*, and *utility functions*. A player has various actions to choose from. After all players choose the actions simultaneously, the outcome of the game is decided, and their utilities are denoted by the utility functions with the outcome as input. To maximize a player's utility, he applies a *strategy* to choose specific actions under predefined conditions. Note that one's applied strategy may influence others' utilities and make them change their strategies as well, which results in the instability of the system.

In the stable state of the game, any player should have chosen their *best response* to other players' currently applied strategies. If any single player is asked to change his strategy while others' remain unchanged, he sticks to his current strategy because changing his strategy decreases or makes no difference to his utility. This specified strategy combination forms a *Nash Equilibrium* (NE).

Definition 2 (Nash Equilibrium): In a Nash game with a player set P, each player p_i with a strategy space S_i and a utility function u_i, a strategy combination $s^* = \{s_1^*, s_2^*, \ldots, s_n^*\}$ is a Nash Equilibrium if and only if $\forall p_i \in P, \forall s_i \in S_i$

$$u_i(s_i^*, s_{-i}^*) \geq u_i(s_i, s_{-i}^*)$$

where s_{-i}^* is the strategy combination $\{s_j^* | j \neq i\}$.

In addition, there is a special type of NE called *dominant-strategy Nash Equilibrium* (DSNE). In DSNE, given any combination of other players' strategies, a player's best response is always the same. Since a player's best response now is independent of other players' strategies, the implementation complexity is greatly reduced.

Definition 3 (Dominant-Strategy Nash Equilibrium): In a Nash game with a player set P, each player p_i with a strategy space S_i and a utility function u_i, a strategy combination $s^* = \{s_1^*, s_2^*, \ldots, s_n^*\}$ is a dominant-strategy Nash Equilibrium if and only if $\forall p_i \in P, \forall s_i \in S_i, \forall s_{-i} \in S_{-i}$

$$u_i(s_i^*, s_{-i}) \geq u_i(s_i, s_{-i})$$

where s_{-i}^* is the strategy combination $\{s_j^* | j \neq i\}$ and S_{-i} is the strategy space of players despite p_i.

We formulate the femtocell cell-breathing control framework into a two-stage extensive-form Nash Game. Stage 1 is the Cell-Breathing stage, where we implement the femtocell downlink cell-breathing mechanism in order to collect the private information (CQI, as an instance) of MSs. All MSs report their θ to the mechanism in this stage, and then the mechanism chooses P_{f}. Stage 2 is the Cell Selection stage, where MSs select their preferred BS. In both stages, all $M_i \in S$ are the players. Their strategy spaces are $\Theta \times \{M_i \in S_{\mathrm{f}}, M_i \in S_{\mathrm{m}}\}$, where Θ is the set of all possible state of private information in Stage 1, and $M_i \in S_j$ represents its choice in Stage 2.

The choice on utility function depends on the QoS requirements of the MSs. It can relate to the throughput, delay, or even the jitter of the service experienced by the MSs. In this paper, we denote the utility function of M_i by $u_i = \gamma_i$, where γ_i is M_i's expected throughput. This characterizes the MS as a selfish user seeking a higher throughput. Other types of utility functions regarding delay or jitter can be applied too, especially when certain QoS factor is in the information to be reported.

We follow the backward induction procedure to find the NE in the proposed two-stage Nash Game. First, we explore the NE in the Cell Selection subgame (composed of the cell selection stage only) regarding all possible outcomes of the previous stage. Then, we move backward and check the NE in the game (composed of these two stages) given the NEs in the Cell Selection subgame. The NE we derive by following this procedure is a Subgame-Perfect Nash Equilibrium (SPNE).

IV. Nash Equilibrium in Cell Selection Subgame

We first find the NE in the Cell Selection subgame. The following theorem describes the best response of M_i to select the cells under femtocell power p.

Theorem 1: Under the allocation rule $A(\cdot)$ satisfying Assumption 1, M_i's best response in the Cell Selection subgame is

$$\beta_i(p) = \begin{cases} M_i \in S_{\mathrm{f}}, & \text{if } \Gamma_{i,\mathrm{f}}(p) \geq \gamma_{i,\mathrm{m}} \\ M_i \in S_{\mathrm{m}}, & \text{otherwise.} \end{cases} \tag{4}$$

In addition, given the MS set $S_{\mathrm{f}}(p)$ under the downlink power p, $M_i \in S_{\mathrm{f}}(p)$'s expected throughput $\gamma_{i,\mathrm{f}}$ is given as follows:

$$\gamma_{i,\mathrm{f}} = \begin{cases} \Gamma_{i,\mathrm{f}}(p), & \text{if } \Gamma_{i,\mathrm{f}}(p) < \gamma_{\mathrm{f}}(p) \\ \gamma_{\mathrm{f}}(p), & \text{otherwise} \end{cases} \tag{5}$$

where

$$\begin{aligned} \sum_{M_i \in S_{\mathrm{f}}^u(p)} \Gamma_{i,\mathrm{f}}(p) + |S_{\mathrm{f}}^c(p)|\gamma_{\mathrm{f}}(p) &= \min\{C_{\mathrm{f}}, \sum_{M_i \in S_{\mathrm{f}}(p)} \Gamma_{i,\mathrm{f}}(p)\} \\ S_{\mathrm{f}}^u(p) &= \{M_i | \Gamma_{i,\mathrm{f}}(p) < \gamma_{\mathrm{f}}(p)\} \\ S_{\mathrm{f}}^c(p) &= S_{\mathrm{f}}(p) \setminus S_{\mathrm{f}}^u(p). \end{aligned} \tag{6}$$

Note that the best response of M_i is independent of other MSs' strategies. Thus, these best responses form a unique DSNE in the Cell Selection subgame: Each MS chooses to connect to the cell that offers the higher wireless data rate. This expected behavior is similar to the cell selection procedure in legacy wireless devices.

In the Cell-Breathing stage, as we discussed in Section II, the cell-breathing rule should be truthful in order to prevent cheating behavior in MSs.

Definition 4 (Truthful Rule): A downlink cell-breathing rule $B(\bar{\theta})$ under $A(\{\Gamma(\eta_{i,\mathrm{f}}) | M_i \in S_{\mathrm{f}}\})$ is truthful if $\forall M_i \in S_{\mathrm{f}}$ with their true information $\bar{\theta}^*$, and $\forall \bar{\theta} \in \Theta^n$, $u_i(\gamma_{i,\mathrm{f}}^*) \geq u_i(\gamma_{i,\mathrm{f}})$, where $\{\gamma_{i,\mathrm{f}}^{(*)}\} = A(\{\Gamma_{i,\mathrm{f}}(B(\bar{\theta}^{(*)}))\})$.

As shown in the definition, the truthful strategies in fact construct an NE since no user will deviate from the truthful strategy.

Here, we show the truthfulness of the Virtual Election rule. The Virtual Election rule is based on MVS, which has been shown truthful when the preferences of voters are single-peaked preferences [25].

Definition 5 (Single-Peaked Preference): A preference $\succeq$ over $\bar{R}$ is single-peaked if and only if there exists a unique $\bar{r_i} \in \bar{R}$ that $\forall r \in \bar{R} \setminus \{\bar{r_i}\}$ and $\forall \theta \in [0, 1)$, $\theta r + (1 - \theta)\bar{r_i} \succeq r$, where $i \succeq j$ represents i is preferred or equal to j for the player.

It has been proved by Ching [26] that all voters will vote for their peak choice $\bar{r_i}$ in MVS when their preferences are single-peaked. Thus, MVS is a truthful rule since all voters report their most preferred choices truthfully. Recalling the Virtual Election scheme rule in (1), if $L_{i,j}|_{j=\{\mathrm{f},\mathrm{m}\}}$ is public information among MSs, that is, all MSs know other MSs' CQI, it can be proved that the preference of MSs on the femtocell

downlink power is single-peaked when the allocation rule $A(\cdot)$ satisfies Assumption 1. We first provide an insight of this preference characteristic: For $M_i \in S_{\rm f}$ served by the femtocell BS, its expected throughput $\gamma_{i,{\rm f}}$ is decided by the allocation rule $A(\cdot)$, which takes the MS set $S_{\rm f}$ and their wireless data rates $\{\Gamma_{i,{\rm f}}(P_{\rm f})\}$ as inputs. Both inputs of $A(\cdot)$ are affected by the choice of downlink power $P_{\rm f}$ of the femtocell BS. A higher $P_{\rm f}$ will encourage more MSs connect to the femtocell and therefore share femtocell BS's backhaul capacity. This decreases the expected throughput of each MS. Nevertheless, a higher $P_{\rm f}$ also enhances the transmission qualities of MSs by increasing the wireless data rate and therefore relaxing the expected throughput constraint. This may bring a higher expected throughput for the MS if its expected throughput is constrained by the wireless data rate. Along with the changes of $P_{\rm f}$, these two inputs have opposite effects on the expected throughput to MSs. Note that if the macrocell and femtocell share the same spectrum, the conflicting effect of these two inputs becomes more significant. For instance, when the femtocell uses a higher downlink transmission power, the interference to the macrocell is stronger. The increased interference may encourage more MSs to choose femtocell as their serving cell. Thus, more MSs share the limited backhaul capacity, and their expected throughput under the femtocell is decreased.

Formally, we define each MS's preference over $P_{\rm f}$:

Definition 6 (MS's Preference on $P_{\rm f}$): M_i's preference over $P_{\rm f}$ is denoted as $\succeq_i$, which satisfies

$$\forall p, p' \in [0, P_{\rm f}^{\max}],\ p \succeq_i p' \Leftrightarrow u_i(A_i(p)) \geq u_i(A_i(p'))$$

where $\{\gamma_{i,{\rm f}}\} = A(\{\Gamma_{i,{\rm f}}(p)\})$ and $A_i(p) = \gamma_{i,{\rm f}}$.

The following theorem shows that for a given $\succeq_i$, there exists an ideal p_i^* that is preferred or equal to any other choices of $p \in [0, P_{\rm f}^{\max}]$. Thus, $\succeq_i$ is a single-peaked preference with a peak choice p_i^*.

Theorem 2 (Single-Peaked Preference on $P_{\rm f}$): When the allocation rule $A(\cdot)$ satisfies Assumption 1, $\forall M_i \in S_{\rm f}$, $\succeq_i$ is single-peaked with peak p_i^*, where p_i^* is denoted as

$$p_i^* = \begin{cases} P^{\rm F}, & i = \arg\max_{M_i \in S}\{L_{i,{\rm f}}\} \\ P_i^{\rm M}, & \text{otherwise} \end{cases} \tag{7}$$

where

$$P^{\rm F} = \begin{cases} \Gamma_{\rm f}^{-1}(C_{\rm f}), & \text{if } \Gamma_{\rm f}^{-1}(C_{\rm f}) \text{ exists} \\ p_j^{b-}, & \text{otherwise.} \end{cases} \tag{8}$$

$$P_i^{\rm M} = \min\{\arg_p(\Gamma_{i,{\rm f}}(p) = \gamma_{\rm f}(p)), P_{\rm f}^{\max}\} \tag{9}$$

$p_i^b = \Gamma_{i,{\rm f}}^{-1}(\gamma_{i,{\rm m}})$, $C_{\rm f} - \gamma_{j,{\rm m}} < \Gamma_{\rm f}(p_j^{b-}) < C_{\rm f}$, and $\Gamma_{\rm f}(p) = \sum_{p_i^b \leq p} \Gamma_{i,{\rm f}}(p)$.

Thus, under a given allocation rule $A(\cdot)$ satisfying Assumption 1, MSs with good channel qualities prefer $P^{\rm F}$, which is the minimum femtocell downlink power to maximizes the overall expected throughput of MSs under the femtocell. If $P^{\rm f}$ is increased, more users connect to the femtocell, and their expected throughput is strictly decreased. For those MSs with poor channel qualities, each of them prefers a femtocell downlink power that maximizes their own expected throughput. If we assume a shared spectrum model, the conflicting effect of two inputs on the allocation rule is more significant, and the single-peakedness of user's preferences on $P_{\rm f}$ will be held in the shared spectrum model, despite the peak powers being different from those described in Theorem 2. In detail, in the shared spectrum model, the expected throughput of M_i under macrocell $\gamma_{i,{\rm m}}$ should be decreasing with $P_{\rm f}$ due to the interference from the femtocell. Therefore, we may define a decreasing function $\Gamma_{i,{\rm m}}(P_{\rm f})$ to represent M_i's expected throughput under macrocell. Nevertheless, two important observations in the independent spectrum model are still valid: 1) The wireless data rate under femtocell $\Gamma_{i,{\rm f}}(P_{\rm f})$ remains an increasing function of $P_{\rm f}$ since the macrocell does not change its transmission power and the interference from the macrocell is therefore nonincreasing with $P_{\rm f}$. 2) There is at most one boundary point $P_{\rm f}^*$ that $\Gamma_{i,{\rm m}}(P_{\rm f}) = \Gamma_{i,{\rm f}}(P_{\rm f})$ for every $M_i \in S$ since the former one is a decreasing function while the latter one is an increasing function. Supporting by these two observations, the conclusions in Theorems 1 and 2 remain valid in the shared spectrum model.

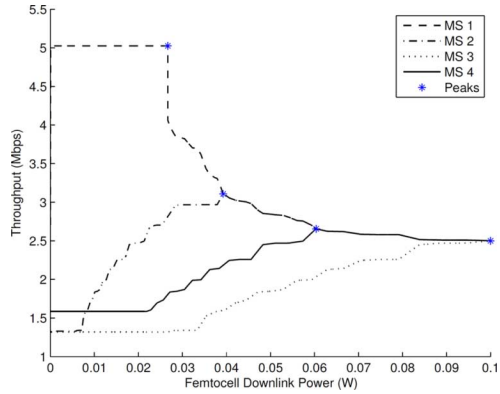

Fig. 3. MSs' single-peaked preferences over $P_{\rm f}$.

An example of the preferences of MSs with corresponding expected throughput is shown in Fig. 3. Four MSs are in the overlay network, and the femtocell's backhaul data rate is 7 Mb/s. Using MS 2's data rate as an example, the downlink power that maximizes its expected throughput is 0.3926 W. Its data rate strictly decreases when the power increases or decreases. Thus, its peaked power $p_2^* = 0.3926$.

Since MSs' preferences are single-peaked, we give a corollary to conclude the truthfulness of the Virtual Election rule.

Corollary 3 (Truthfulness of Virtual Election Rule): The Virtual Election rule is a truthful rule when the allocation rule $A(\cdot)$ satisfies Assumption 1.

Proof: Returning to the Virtual Election rule, because the MSs' preferences over $P_{\rm f}$ are single-peaked, M_i will choose to report its most preferred power p_i^* under the Virtual Election rule. Therefore, the Virtual Election rule is truthful. □

V. FEVER Mechanism

Although the Virtual Election rule can make MSs truthfully report their preferences on downlink power, the NE in the Virtual Election rule is not a DSNE since the peak value p_i^* of M_i depends on the channel qualities of other MSs. Thus, there is a serious drawback in the mechanism: All MSs and the femtocell are required to possess complete information of other MSs such as their signal-loss rates and interference levels in order to derive the peak p_i^*. This requirement is undesirable in a realistic wireless network since the implementation of information sharing among MSs induces a huge overhead. Hence, we

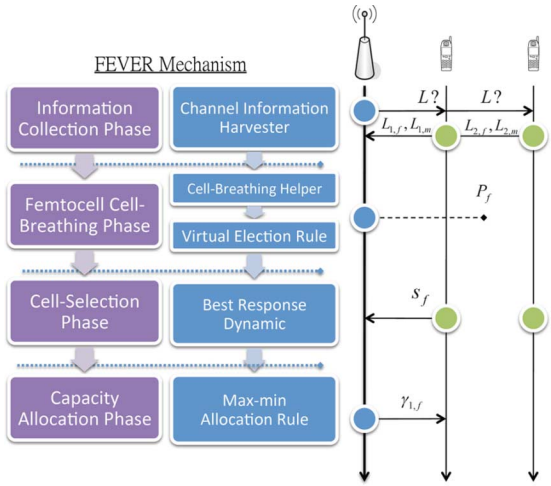

Fig. 4. FEVER mechanism.

propose the FEVER mechanism for the cell-breathing control framework. FEVER is a truthful mechanism based on the Virtual Election rule without the requirement of complete information. MSs are only required to report their information directly to the femtocell without calculating their preferred downlink power. In addition, we prove that there exists a truthful DSNE in the FEVER mechanism. Therefore, the truthfulness of FEVER is guaranteed with lower implementation complexity.

As shown in Fig. 4, the FEVER mechanism is composed of three levels in the Cell-Breathing stage: Channel Information Harvester (CIH), Cell-Breathing Helper (CBH), and Virtual Election Rule (VER). First, CIH requires all MSs to report their information $\theta_i \in \Theta$. The choice of reported information depends on the QoS information with which we are concerned. In this paper, we choose $\theta_i \equiv \{L_{i,\mathrm{f}}, L_{i,\mathrm{m}}\}$ and therefore $\Theta \equiv \Lambda \times \Lambda$ since CQI is the most important QoS information to influence the throughput. Other QoS information such as delay constraints are applicable. For example, when the utility function of the MS is related to the delay experienced by the MS, the delay constraints of the MSs should be included in the QoS information here.

Then, CBH uses the channel information harvested by CIH to calculate MSs' most preferred downlink power p_i^*. These values are derived by $H(\{\theta_i | M_i \in S\}) = H(\bar{\theta}) = \{p_i^* | M_i \in S\}$, where $H(\cdot)$ is in accordance with the results given by (7). Finally, VER collects $\{p_i^* | M_i \in S\}$ derived from CBH and applies the Virtual Election rule to choose the femtocell downlink power P_{f}. Then, in the Cell Selection stage, there are two levels: BEst response Dynamic (BED) and Max-min Allocation Rule (MAR). According to the chosen P_{f}, MSs select the cell they want to be served by, which can be predicted by Theorem 1. Thus, S_{f} and S_{m} are decided in this level. Since we have all CQI from CIH, we induce a cheat-proof procedure here: If an MS M_j that is not in $S_{\mathrm{f}}(P_{\mathrm{f}})$ calculated by CBH selects the femtocell in this stage, we surely know this MS is cheating in the Cell-Breathing stage, and thus we can block this MS from using the femtocell service. Finally, the femtocell allocates the backhaul data rate according to the max-min allocation rule $A_{\mathrm{fever}}(\cdot)$.

Then, we give the following theorem to show the truthfulness of the FEVER mechanism.

Theorem 4 (Truthfulness of FEVER Mechanism): All M_i report their CQI $\theta_i^* = \{\mathrm{L}_{i,\mathrm{f}}^*, \mathrm{L}_{i,\mathrm{m}}^*\}$ truthfully in the FEVER mechanism $B_{\mathrm{fever}}(\cdot)$. That is, $\forall M_i \in S, \forall \bar{\theta} \in \Theta^n = (L \times L)^n$

$$u_i(A_i(B_{\mathrm{fever}}(\bar{\theta}^*))) \geq u_i(A_i(B_{\mathrm{fever}}(\bar{\theta}))).$$

Proof: Due to page limitation, we sketch the outline of the proof here. We discuss three cases: M_i's vote v_i derived in CIH is equal to, larger than, or smaller than the selected vote v_κ. For the first case, surely M_i will just report its CQI truthfully. For the second case, the vote chosen by FEVER is larger than its most preferred downlink power v_i. Therefore, $\gamma_{i,\mathrm{f}} = \Gamma_{\mathrm{f}}(v_\kappa)$ according to Assumption 1 and Theorem 2. If M_i chooses to report $L'_{i,\mathrm{f}} < L^*_{i,\mathrm{f}}$, the modified vote v'_i will be larger than v_i, and the vote chosen by VER v'_κ will be no smaller than v_κ according to VER. Thus, $\gamma'_{i,\mathrm{f}} = \Gamma_{\mathrm{f}}(v'_\kappa) \leq \Gamma_{\mathrm{f}}(v_\kappa)$. Since it eventually gets a lower downlink data rate, it has no incentive to report $L'_{i,\mathrm{f}} < L^*_{i,\mathrm{f}}$. However, if M_i chooses to report $L'_{i,\mathrm{f}} > L^*_{i,\mathrm{f}}$, since the modified vote v'_i will be smaller than v_i, and the original selected vote v_κ is larger than v_i, reporting $L'_{i,\mathrm{f}}$ makes no difference to v_κ. Additionally, since $\gamma_{i,\mathrm{f}}$ is already not constrained by its wireless data rate $\Gamma_{i,\mathrm{f}}(v_\kappa)$, its downlink data rate remains the same $\gamma'_{i,\mathrm{f}} = \Gamma_{\mathrm{f}}(v_\kappa) = \gamma_{i,\mathrm{f}}$. Therefore, it has no incentive to report $L'_{i,\mathrm{f}} > L^*_{i,\mathrm{f}}$. Similarly, in the third case, M_i still chooses to report $L^*_{i,\mathrm{f}}$. For $L_{i,\mathrm{m}}$, given $M_i \in S_j$ if v_κ is selected and $L^*_{i,\mathrm{m}}$ is reported, it makes no difference to v_κ unless given the reported $L'_{i,\mathrm{m}}$, M_i will make a choice of $S'_j \neq S_j|_{j=\{\mathrm{f},\mathrm{m}\}}$. However, since M_i's true CQI is $L^*_{i,\mathrm{m}}$, it will choose S_j in the Cell Selection stage, and thus the cheating will be revealed by the femtocell. Hence, the FEVER mechanism is a truthful mechanism. Note that this proof requires that the capacity assumption is satisfied or $\Gamma_{\mathrm{f}}(p)$ may not be a decreasing function. □

Notice that the proof is not limited to CQI case but can be generalized to other type of QoS information. The key point here is when the single-peaked preferences on S_{f} is guaranteed if certain QoS-based utility function u_i is chosen, the FEVER mechanism guarantees that the related QoS information will be truthfully reported.

If the capacity assumption, that is, $\forall M_i \in S$, $\frac{C_{\mathrm{f}}}{N} \geq \gamma_{i,\mathrm{m}}$, is not satisfied, the preference on power is no longer single-peaked. However, the FEVER mechanism is still truthful when the selected vote order κ is equal to 1. We show this characteristic in the following theorem.

Theorem 5 (Truthfulness Without Capacity Assumption): When $\exists M_i \in S$, $\frac{C_{\mathrm{f}}}{N} < \gamma_{i,\mathrm{m}}$, all M_i still report their CQI $\theta_i^* = \{\mathrm{L}_{i,\mathrm{f}}^*, \mathrm{L}_{i,\mathrm{m}}^*\}$ truthfully in the FEVER mechanism $B_{\mathrm{fever}}(\cdot)$ when selected vote order $\kappa = 1$.

Proof: Since $\kappa = 1$, $\forall M_i \in S_{\mathrm{f}}, \gamma_{i,\mathrm{f}} = \Gamma_{i,\mathrm{f}}(v_1)$. For a given $M_j \in S_{\mathrm{f}}$, if it chooses to report $\mathrm{L}'_{i,\mathrm{f}} < \mathrm{L}^*_{i,\mathrm{f}}$, its allocated data rate $\Gamma'_{i,\mathrm{f}}$ is strictly lower than $\Gamma_{i,\mathrm{f}}$ because it claims a lower wireless data rate. In contrast, if it chooses to report $\mathrm{L}'_{i,\mathrm{f}} > \mathrm{L}^*_{i,\mathrm{f}}$, it claims a higher wireless data rate, and the CBH will decide a lower vote $v'_1 < v_1$, and thus its real downlink data rate $\gamma_{i,\mathrm{f}} = \Gamma(v'_1 \mathrm{L}^*_{i,\mathrm{f}}) < \Gamma(v'_1 \mathrm{L}^*_{i,\mathrm{f}})$. Thus, it will truthfully report $\mathrm{L}_{i,\mathrm{f}}$. For $\mathrm{L}^*_{i,\mathrm{m}}$, a misreported $\mathrm{L}'_{i,\mathrm{m}}$ does not affect the vote v_1 unless it is large enough that the MS will not be counted in S_{f} in CBH. According to the cheat-proof procedure in BED, this MS cannot return to the femtocell, and its downlink data rate is $\gamma_{i,\mathrm{m}} < \Gamma_{i,\mathrm{f}}(v_1)$. Hence, $\forall M_i \in S_{\mathrm{f}}$, they all report CQI θ_i^*. Similarly, $\forall M_j \in S_{\mathrm{m}}$, they also report CQI θ_j^*. Thus, the

FEVER mechanism is truthful even when $\exists M_i \in S$, $\frac{C_\mathrm{f}}{N} < \gamma_{i,\mathrm{m}}$. □

The choice of $\kappa = 1$ not only relaxes the capacity assumption, but also makes the FEVER mechanism choose the most capacity-efficient operation point in most network scenarios, which will be shown in Section V-A.

A. Performance Analysis of FEVER Mechanism

In the FEVER mechanism, the selected vote order κ is predefined in VER to derive the κth votes as the choice of P_f. Now we discuss the influence of κ on the (throughput) efficiency and (allocation) fairness of the resulting expected throughput $\{\gamma_{i,\mathrm{f}}|M_i \in S_\mathrm{f}\}$ and $\{\gamma_{i,\mathrm{m}}|M_i \in S_\mathrm{m}\}$. We will show that there is a tradeoff between efficiency and fairness when different κ is chosen.

1) Price of Anarchy: First we define the price of anarchy (POA): the ratio of the maximum social utility to the social utility at NE. POA is used to measure the efficiency loss due to the selfish behavior of MSs in NE. If POA is equal to one, there is no efficiency loss at NE, and NE leads to the same performance as the social-utility maximized system. In the femtocell cell-breathing control framework, we define the social utility as $U_\mathrm{s} = \sum_{M_i \in S} u_i$. The price of anarchy of the FEVER mechanism is described as follows.

Theorem 6: The price of anarchy of the FEVER mechanism $POA(\kappa)$ is one if the selected vote order $\kappa = 1$ and the social-utility maximized power P_f^* can be described as

$$\sum_{i=1}^{j} \Gamma(P_\mathrm{f}^* L_{i,\mathrm{f}}) \le C_\mathrm{f} \quad \text{and} \quad \sum_{i=1}^{j+1} \Gamma(P_\mathrm{f}^* L_{i,\mathrm{f}}) \ge C_\mathrm{f}.$$

In addition, $POA(\kappa)$ is increasing with κ and bounded by 2.

Proof: First, we shortly describe how to find the optimal downlink power in the femtocell: We first sort MSs in increasing order of $\frac{L_{1,\mathrm{m}}}{L_{1,\mathrm{f}}}$. (This guarantees that MSs join the femtocell sequentially when the femtocell BS increases P_f.) Intuitively, the optimal power that maximizes social utility is the one that just allocates all the available backbone capacity to MSs. If the solution does not exist and the macrocell's data rate is relatively large, the optimal power will be the one that minimizes the unallocated backbone data rate before an additional MS joins S_f and uses all the capacity. Thus, the optimal power P_f^* is given by $\sum_{i=1}^{j} \Gamma(P_\mathrm{f}^* L_{i,\mathrm{f}}) \le C_\mathrm{f}$ and $\sum_{i=1}^{j+1} \Gamma(P_\mathrm{f}^* L_{i,\mathrm{f}}) > C_\mathrm{f}$, where j satisfies $P_\mathrm{f}^* L_{i,\mathrm{f}} \ge P_\mathrm{m} L_{i,\mathrm{m}}$, $\forall i \le j$ and $P_\mathrm{f}^* L_{i,\mathrm{f}} < P_\mathrm{m} L_{i,\mathrm{m}}$ $\forall i \ge j$. If $\sum_{i=1}^{j} \Gamma(P_\mathrm{f}^* L_{i,\mathrm{f}}) = C_\mathrm{f}$, the social utility $U_\mathrm{s}^* = \sum_{M_i \in S} u_i = C_\mathrm{f} + \sum_{i=j+1}^{N} \Gamma_{i,\mathrm{m}}$. We observe that P_f, which is the peak value of M_1, is equal to P_f according to Theorem 2. Thus, if $\kappa = 1$, the FEVER mechanism always chooses P_f^*, and $POA(1) = 1$. The reason that $POA(\kappa)$ is an increasing function is intuitive. When P_f increases, there are two possible cases: JOne is that a new MS M_j joins S_f, and the other is that no MS changes its selection. For the former case, the social utility will decrease by $\gamma_{j,\mathrm{m}}$ since M_j chooses to join S_f and gives up the throughput offered by the macrocell. For the latter case, there is no change in the resulting social utility. In addition, we know v_κ increases with κ, so $P_\mathrm{f} = B_{\mathrm{fever}}(\cdot, \kappa)$ is an increasing function of κ. Thus, $POA(\kappa)$ is an increasing function of κ.

Finally, since the worst case in the FEVER mechanism will be that all users choose to join the femtocell and all macrocell's offered services are wasted under selfish behavior, we have $\gamma_{i,\mathrm{f}}|_{\kappa=N} > \gamma_{i,\mathrm{m}}$ $\forall M_i \in S$. In addition, we know $\sum M_i \in S \gamma_{i,\mathrm{f}}|_{\kappa=N} = C_\mathrm{f}$. Thus, $POA(\kappa) \le POA(N) = \frac{C_\mathrm{f} + \sum_{M_i \in S_\mathrm{m}(P_\mathrm{f}^*)} \gamma_{i,\mathrm{m}}}{C_\mathrm{f}} < \frac{C_\mathrm{f} + C_\mathrm{f}}{C_\mathrm{f}} = 2$. □

Theorem 6 tells us that when $\kappa = 1$, the FEVER mechanism always chooses the downlink power that maximizes the social utility. In addition, according to Theorem 5, even if the capacity assumption is relaxed, the FEVER mechanism can still maximize the social utility because all MSs truthfully report their CQI when $\kappa = 1$. For $\kappa > 1$, the social utility decreases with κ since more MSs join S_j and waste the throughput offered by the macrocell. Thus, the output becomes inefficient.

Note that, in some scenarios, the optimal power P_f^* may not be the one described in Theorem 6. This happens when $\gamma_{j+1,\mathrm{m}} < C_\mathrm{f} - \sum_{i=1}^{j} \Gamma(P_\mathrm{f}^* L_{i,\mathrm{f}})$. In this case, allowing M_{j+1} to join the femtocell is beneficial to the system since the unallocated backhaul capacity is significantly large. In this case, $POA(1)$ will be slightly larger than one. The degree of efficiency loss depends on the macrocell downlink data rate of $\gamma_{j,\mathrm{m}}$. Given $\gamma_{j,\mathrm{m}}$, $POA(1) < \frac{C_\mathrm{f} + \gamma_{j,\mathrm{m}}}{C_\mathrm{f}} = 1 + \frac{\gamma_{j,\mathrm{m}}}{C_\mathrm{f}}$. If capacity assumption is satisfied, $POA(1) < 1 + \frac{1}{N}$.

2) Fairness: Then, we discuss the fairness among $M_i \in S$ when κ changes. Since the allocation rule $A_{\mathrm{fever}}(\cdot)$ follows Assumption 1, the resource allocation (backhaul capacity) among all MSs in S_f surely satisfies max-min fairness. In addition, given a predetermined κ, all MSs' utilities satisfy the max-min fairness under the FEVER mechanism.

Theorem 7: Given κ, all MSs' utilities $\{u_i|M_i \in S\}$ under the FEVER mechanism satisfy max-min fairness, that is

$$\exists \{u_i'\} \ne \{u_i\}, u_k' > u_k \text{ for some } M_k \in S \Rightarrow \exists M_i \in S,\ u_i' < u_i \le u_k.$$

Here, we would like to further discuss the fairness efficiency among all MSs in the overlay system. To discuss the fairness efficiency, we apply a common fairness index: Jain fairness index $I(\{u_i\}) = \frac{(\sum_{1 \le i \le N} u_i)^2}{N \sum_{1 \le i \le N} u_i^2}$ [27] here. Jain fairness index is bounded between 0 and 1. A higher fairness index means the resource allocation is fairer. The following theorem describes the fairness efficiency of the FEVER mechanism.

Theorem 8: The fairness index $I(\{u_i\})$ of output of the FEVER mechanism is an increasing function of κ.

Proof: We use [27, Property 1] to prove this. Before that, we define the reallocation sequence $\{(M_i^1, M_j^1, du_1), (M_i^2, M_j^2, du_2), \ldots\}$, where (M_i^l, M_j^l, du^l) means M_i^l's utility (downlink data rate) minus du^l while M_j^l's utility plus du^1. We also recall the notations $S_\mathrm{f}^u(p)$ and $S_\mathrm{f}^c(p)$ in the proof of Theorem 1 in the Appendix.

According to Theorem 1, for a given p and $p' = dp + p > p$, we have $S_\mathrm{f}(p) \subset S_\mathrm{f}(p')$ and $\gamma_\mathrm{f}(p) > \gamma_\mathrm{f}(p')$. Without losing generality, we assume dp is small enough that only one of the following cases happens when power is increased to p': $S_\mathrm{f}(p') = S_\mathrm{f}(p)$ or $S_\mathrm{f}(p') = S_\mathrm{f}(p) \cup \{MS_j\}$.

Since the reallocation only happens in MSs in $S_\mathrm{f}(p')$, we focus on the effect of these users and ignore users served by the macrocell. For the first case, no new MS joins $S_\mathrm{f}(p')$. Since $\sum_{M_i \in S_\mathrm{f}(p')} u_i = \sum_{M_i \in S_\mathrm{f}(p)} u_i = C_\mathrm{f}$ and $\gamma_\mathrm{f}(p) > \gamma_\mathrm{f}(p')$,

there exists at least one reallocation sequence $\{(M_i^l, M_j^l, du^l)\}$, where $M_i^l \in S_{\rm f}^c(p)$ and $M_j^l \in S_{\rm f}^u(p')$ can realize the reallocation from $\{\gamma_{i,{\rm f}}(p)\}$ to $\{\gamma_{i,{\rm f}}(p')\}$.

According to the proof of Theorem 1 in the Appendix, $\forall M_i \in S_{\rm f}^c(p)$, $\gamma_{i,{\rm f}}(p') = \gamma_{\rm f}(p') < \gamma_{\rm f}(p)$. Also, $\forall M_j \in S_{\rm f}^u(p')$, $\gamma_{j,{\rm f}}(p) \leq \gamma_{j,{\rm f}}(p') \leq \gamma_{\rm f}(p')$. Thus, for all reallocation (M_i^l, M_j^l, du^l), $du^l \leq \gamma_{i^l,{\rm f}}(p) - \gamma_{i^l,{\rm f}}(p') = \gamma_{i^l,{\rm f}}(p) - \gamma(p') \leq \gamma_{i^l,{\rm f}}(p) - \gamma_{j^l,{\rm f}}(p) = u_i^l(p) - u_j^l(p)$.

According to [27, Property 1], Jain fairness index increases when $du \leq u_i - u_j$. This means after every reallocation (M_i^l, M_j^l, du^l), Jain fairness index increases. Thus, the final output $I(\{u_i(p')\})$ is larger than $I(\{u_i(p')\})$ when $p' > p$ in the first case. Similarly, In the second case, we can reach the same conclusion. Thus, the fairness index of the output of the FEVER mechanism is an increasing function of femtocell downlink power p. Finally, since v_κ is increasing with κ, $I(\kappa) = I(\{u_i(v_\kappa)\})$ is increasing with κ. □

Notice that when $\kappa = N$ and $p_N^* \leq P_{\rm f}^{\max}$, the output of the FEVER mechanism has a fairness index of one.

Observed in Theorems 6 and 8, there is a tradeoff between throughput efficiency and allocation fairness. The choice of κ should be application-oriented. On one hand, if the service provider wants to make use of the additional backhaul data rate offered by the femtocell efficiently, he can choose a smaller κ. On the other hand, if he wants to make users share the backhaul fairly, he may choose a larger κ.

VI. Subscriber Group Modes

We now investigate the compatibility of the FEVER mechanism to subscriber group modes in a femtocell system. In implementing the subscriber group modes in femtocells, two issues are of concern: access control on low-priority MSs and resource reservation for high-priority MSs. These two concerns change the access policy of femtocells and may bring some incompatibility to existing access policies for typical cell base stations.

We first apply necessary extensions into our downlink cell-breathing framework and two-stage game model. We add a new phase: Access Control Phase between Cell Breathing and Cell Selection phases into the framework. In this phase, the femtocell should decide and broadcast the allowed mobile user set $S^{\rm a}$. Only users in $S^{\rm a}$ are allowed to access the femtocell. Notice that the choice of $S^{\rm a}$ depends on the subscriber group mode and the available resource.

To model the user behavior in the new framework, we extend the two-stage game model in Section III. The Access Control Phase is included in the first stage (Cell-Breathing Stage) of our two-stage game model. In the new game model, the Cell-Breathing rule is extended to output not only the femtocell downlink power $P_{\rm f}$, but also the allowed mobile user set $S_{\rm a}$. In addition, in the Cell-Selection stage, we impose a new game rule: Only users belonging to $S_{\rm a}$ have the right to access the femtocell. Mathematically, the player set in the second stage is now restricted to $S^{\rm a}$ instead of S. Other users $M_i \notin S^{\rm a}$ can only select the macrocell. In the femtocell, a subscriber group $S^{\rm g} \subset S$ is predetermined. Each MS $M_i \in S^{\rm g}$ has a desired expected throughput $\gamma_i^{\rm req}$. We assume their utility is maximized whenever the desired rate is satisfied. Thus, the utility function of $M_i \in S^{\rm g}$ is $u_i(\gamma) = \min(\gamma, \gamma_i^{\rm req})$. Lastly, we assume the backhaul data rate can support at least the demand of these MSs, that is, $C_{\rm f} \geq \sum_{M_i \in S^{\rm g}} \gamma_i^{\rm req}$. With this assumption, we define the reserved capacity function $C^{\rm g}(p)$

$$C^{\rm g}(p) = \sum_{M_i \in S^{\rm g,a}(p)} (\min(\Gamma_{i,{\rm f}}(p), \gamma_i^{\rm req})) \tag{10}$$

where $M_i \in S^{\rm g,a}(p)$ if and only if $M_i \in S^{\rm g}$ and $\Gamma_{i,{\rm f}}(p) \geq \Gamma_{i,{\rm m}}$. $C^{\rm g}(p)$ is the backhaul data rate reserved for users in $S^{\rm g}$. Notice that the assumption and reserved data rate imply that when all users in $S^{\rm g}$ select the femtocell, they all can still have a reasonable service quality. For other users, they may have an unacceptable (lower than the one provided by macrocell) expected throughput if users in $S^{\rm g}$ have higher priority.

A. SG-FEVER Mechanism

We now propose the Subscriber Group FEVER mechanism, a voting-based truthful mechanism that is compatible to three subscriber group modes. Similar to the FEVER mechanism, SG-FEVER is composed of three levels in the Cell-Breathing stage: Channel Information Harvester (CIH), Subscriber Group Cell-Breathing Helper (SG-CBH), and Subscriber Group Virtual Election Rule (SG-VER).

In SG-CBH, instead of directly applying max-min allocation rule to derive the peak of each user, we first define $S^{\rm g,a}(p)$ and $C^{\rm g}(p)$ according to (10). Then, the max-min allocation rule $A_{\rm fever}(\cdot)$ is applied to these two groups independently: The reserved capacity $C^{\rm g}(p)$ is used for users in $S^{\rm g,a}(p)$, while the remaining capacity $C^{-{\rm g}}(p) = C_{\rm f} - C^{\rm g}(p)$ is used for users in $S^{-{\rm g}}(p)$, which is given by

$$S^{-{\rm g}}(p) = \{M_i | \Gamma_{i,{\rm f}}(p) \geq \Gamma_{i,{\rm m}} \text{ and } M_i \notin S^{\rm g}\}.$$

The peak p_i^* and the wireless data rate $\Gamma_{i,{\rm f}}(p)$ of each user $M_i \in S$ are derived in this process.

Finally, SG-VER collects $\{p_i^* | M_i \in S\}$ derived from CBH and applies the Virtual Election rule to choose the femtocell downlink power $P_{\rm f}$ with a predetermined selected vote order κ. In addition, SG-VER broadcasts the allowed user set $S^{\rm a}$, which depends on the choice of subscriber group mode.

Then, in the Cell Selection stage, there are still two levels: BEst response Dynamic (BED) and Subscriber Group Max-min Allocation Rule (SG-MAR). In the SG-FEVER mechanism, MSs select the BS they want to be served by based on their best responses given in Theorem 1 if they are in the allowed user set $S^{\rm a}$. If not, the users have no choice but to choose the macrocell BS as their serving BS. Thus, $S_{\rm f}$ and $S_{\rm m}$ are decided in this level. The cheat-proof procedure in SG-FEVER is enhanced: If an MS not in $S^{\rm g}(P_{\rm f})$ selects the femtocell in this stage, femtocell BS blocks the MS form using femtocell services. Finally, the femtocell allocates the backhaul data rate according to the decision in SG-CBH, and the expected throughput is then determined. Since the implementation of OSG is straightforward, we discuss the implementation of other subscriber group modes.

CSG Mode: In this mode, only users in $S^{\rm g}$ are allowed to access the femtocell. Thus, $S^{\rm a} = \{M_i | \Gamma_{i,{\rm f}}(P_{\rm f}) \geq \gamma_{i,{\rm m}}\} \cap S^{\rm g}$. Note that SG-FEVER promises that users in $S^{\rm g}$ will be allocated at least the wireless data rate $\Gamma_{i,{\rm f}}(P_{\rm f})$ from the femtocell BS, and at most their required throughput $\gamma_i^{\rm req}$. When $\kappa = |S^{\rm g}|$, $\forall M_i \in S^{\rm g}$, $\gamma_{i,{\rm f}}(v_\kappa) = \gamma_i^{\rm req}$. That is, all users derive their required throughput from the femtocell.

Corollary 9 (Truthfulness Under CSG Mode): The SG-FEVER mechanism is a truthful mechanism when S^{g} is nonempty and $S^{\mathrm{a}} = \{M_i | \Gamma_{i,\mathrm{f}}(P_{\mathrm{f}}) \geq \gamma_{i,\mathrm{m}}\} \cap S^{\mathrm{g}}$.

Proof: We first discuss the case that $M_i \notin S^{\mathrm{g}}$. If so, the MS cannot choose the femtocell whatever it reports in SG-CBH since $M_i \notin S^{\mathrm{a}} \subset S^{\mathrm{g}}$. Thus, any $\theta_i \in \Theta$, including θ_i^*, is M_i's best response. Then, if $M_i \in S^{\mathrm{g}}$, since SG-CBH always provides the user at least its raw wireless data rate $\Gamma_{i,\mathrm{f}}(P_{\mathrm{f}})$, its preference on P_{f} is single-peaked with peaks p_i^* at $\Gamma_{i,\mathrm{f}}(p_i^*) = \gamma_i^{\mathrm{req}}$. Hence, M_i will report θ_i^* in the SG-FEVER mechanism. We conclude that reporting θ_i^* is the dominant strategy of any $M_i \in S$ in the SG-FEVER mechanism under CSG mode, that is, SG-FEVER is a truthful mechanism. □

Hybrid Mode: For Hybrid mode, the subscriber group S^{g} is also predefined, but other users are still allowed to access the femtocell if there are remaining resources (backhaul capacity). Given a predetermined nonempty set S^{g}, we define $S^{\mathrm{a}} = \{M_i | \Gamma_{i,\mathrm{f}}(P_{\mathrm{f}}) \geq \gamma_{i,\mathrm{m}}\}$ in this mode. Since we remove the restriction that all users not belonging to S^{g} are excluded from the femtocell, there is a chance that a user $M_i \notin S^{\mathrm{g}}$ will be included in S^{a}. We prove that the SG-FEVER mechanism is a truthful mechanism in Hybrid mode.

Corollary 10 (Truthfulness Under Hybrid Mode): The SG-FEVER mechanism is a truthful mechanism when S^{g} is nonempty and $S^{\mathrm{a}} = \{M_i | \Gamma_{i,\mathrm{f}}(P_{\mathrm{f}}) \geq \gamma_{i,\mathrm{m}}\}$.

Proof: It has been shown in Corollary 9 that $\forall M_i \in S^{\mathrm{g}}$, reporting θ_i^* is their dominant strategy under SG-CBH. Then, $\forall M_i \notin S^{\mathrm{g}}$, the remaining capacity $C^{-\mathrm{g}}(p)$ is allocated according to $A_{\mathrm{fever}}(\cdot)$ in SG-CBH. Thus, according to Theorem 4, their dominant strategy is reporting θ_i^* either. Hence, the SG-FEVER mechanism is a truthful mechanism under Hybrid mode. □

VII. Simulation Results

To evaluate the efficiency and influence of κ in the FEVER mechanism, we implement an LTE overlay macrocell-femtocell simulator by extending the LTE link-level simulator [10]. We follow the settings specified by 3GPP [4] to simulate link-level SINR-throughput results, which are used to specify the wireless data rate function $\Gamma(\cdot)$ in our model. We followed IMT-Advanced 4G evaluation guidelines [9] to construct the overlay macrocell-femtocell system configuration. We apply Outdoor-to-Indoor and Indoor Small Office models as the path-loss models of macrocell signal and femtocell signals, respectively. In our simulations, there are 19 macrocells with a radius of 2 km in hexagonal layout. Within each macrocell, five femtocells are randomly placed. All macrocells share the same carrier, which is different from the one shared by all femtocells. We chose the macrocell in the central and a femtocell at a distance of 1.6 km to the macrocell BS as our simulating overlay system. For MSs within these two cells, their locations are randomly distributed within a 50-m circular house centered at the femtocell BS. All macrocells have a downlink power $P_{\mathrm{m}} = 46$ dBmW, while all background femtocells have a downlink power of 23 dBmW. The additive white Gaussian noise (AWGN) is -132 dBmW. The simulating femtocell has a maximum downlink power limit $P_{\max}^{\mathrm{f}} = 1$ W. The data rate of the femtocell's backhaul C_{f} is 25 Mb/s.

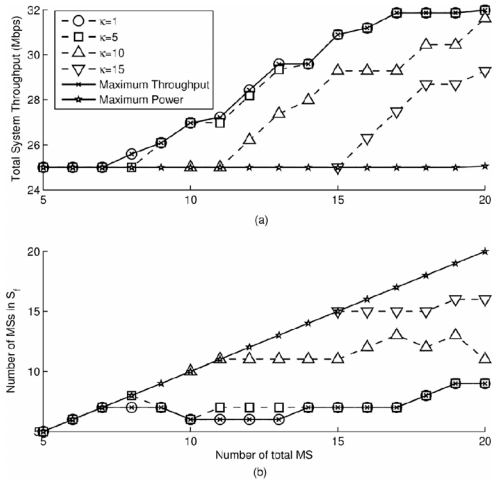

Fig. 5. FEVER mechanism under different choice of κ. (a) Total system throughput. (b) Number of MSs served by femtocell.

A. Effect of MSs on Femtocell Service Range

We first examine the effect of different numbers of MSs on the total system throughput and MSs served by the femtocell. $5 \sim 20$ MSs are randomly placed in the system according to the parameter settings we listed before. We choose four κ settings for the FEVER mechanism: $\kappa = 1$, $\kappa = 5$, $\kappa = 10$, and $\kappa = 15$. For comparison, we also sketch the results of two other mechanisms: Maximum Throughput and Maximum Power. In the Maximum Throughput mechanism, the femtocell chooses the power that maximizes the overall system throughput, that is, $P_{\mathrm{f}} = \arg\max_p \sum_{M_i \in S_{\mathrm{f}}} \gamma_{i,\mathrm{f}} + \sum_{M_i \in S_{\mathrm{m}}} \gamma_{i,\mathrm{m}}$. This mechanism represents the case that the femtocell's objective is maximizing the resource utilization in the system without concerns on the fairness among MSs. In the Maximum Power mechanism, the femtocell always chooses the maximum power $P_{\max}^{\mathrm{f}}$ as its transmission power. This mechanism represents the case that the femtocell's objective is maximizing its coverage in this overlay system. Note that, under both mechanisms, the allocation rule still satisfies Assumption 1, and MSs follow the best responses stated in Theorem 1. Moreover, we assume that the MSs always report their CQI truthfully under the Maximum Throughput mechanism in order to simulate that the femtocell has the perfect knowledge on the current state of wireless system. The results are shown in Fig. 5.

Fig. 5(a) shows that when the number of MSs increases, the total system throughput also increases since more MSs are served by the femtocell or macrocell. We observe that when we choose $\kappa > 1$, the system throughput is lower than the one under $\kappa = 1$. In addition, the system throughput of Maximum Throughput is almost identical as the one under $\kappa = 1$. This observation fits the conclusion in Theorem 6 that $\kappa = 1$ maximizes the total system throughput. For other choices of κ, we observe that a larger κ leads to lower system throughput. In addition, when the number of MSs is small, the FEVER mechanism under large κ chooses the same operating point as the Maximum Power mechanism. This is because for those users who give large votes, they most likely are MSs with poor channel qualities to the femtocell. Thus, they prefer the femtocell power as high as possible. When the number of MSs increases, they then hope the femtocell power is limited

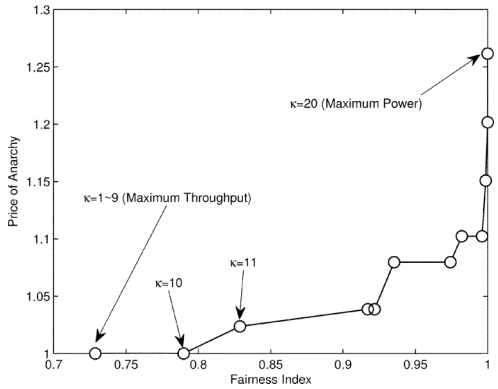

Fig. 6. Efficiency and fairness tradeoff under different choice of κ.

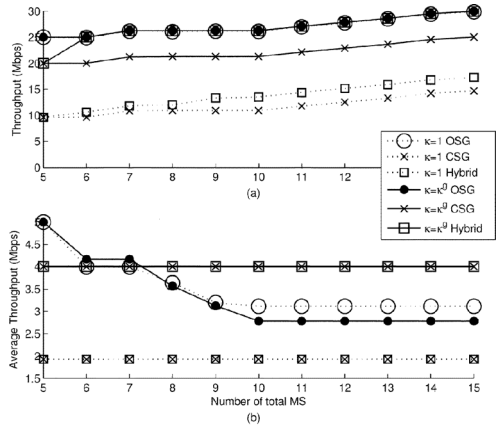

Fig. 7. SG-FEVER mechanism under different subscriber group modes. (a) Total system throughput. (b) Average subscriber group user throughput.

in order to prevent other MSs from joining the femtocell and sharing the limited backhaul capacity.

In Fig. 5(b), we observe that a smaller κ indeed blocks more MSs from joining the femtocell. When the number of total MSs increases, less than 10 MSs are served by the femtocell under $\kappa = 1$. In contrast, more than 15 MSs choose to join S_{f} when $\kappa = 15$. Note that the choice of κ does not necessarily mean that only κ MSs are allowed to join the MSs, but the expected throughput of the v_κ voter is maximized.

B. Tradeoff Between Efficiency and Fairness

Then, we examine the tradeoff between efficiency and fairness when different κ is chosen. Twenty MSs are placed in the overlay system, and we choose $\kappa = 1 \sim 20$ in the experiments. Under each choice of κ, we calculate the system throughput efficiency (the price of anarchy of the FEVER mechanism) and the fairness index of the expected throughput of all MSs. The simulation results are shown in Fig. 6.

The tradeoff between capacity efficiency and allocation fairness is clearly shown in Fig. 6, which fits the conclusion we made in Section V-B. When we choose $\kappa = 1$, the efficiency becomes 1, but the fairness index is 0.7287, which is the lowest one in all operating points. Instead, if we choose $\kappa = 20$, the price of anarchy under the FEVER mechanism becomes 1.2617, and fairness index becomes 1. Note that there may exist multiple choices of κ that lead to the same operating point with the efficiency of 1. This is because some MSs, most likely those near the femtocell BS, have the same votes on P^{F} defined in Theorem 2. In the experiment scenario, there are nine MSs close to the femtocell. They join the femtocell immediately when $P_{\mathrm{f}} > 0$, thus they share the same vote. Hence, all choices of $\kappa < 10$ lead to the same performance, which is the same under the Maximum Throughput mechanism.

C. Influence of Subscribe Group Modes

Finally, we evaluate the influence of different subscriber group modes in overlay system through simulations. Five MSs, which belong to the subscriber group S^{g} and with required throughput of 4Mb/s, are randomly placed in the range between 25–50 m to the femtocell BS. In addition, $0 \sim 10$ MSs are randomly placed in the range between 50–100 m. These MSs are treated as users from outside and do not belong to S^{g}. Then, we apply the SG-FEVER mechanism with two choices of selected vote order: $\kappa = 1$ and $\kappa = \kappa^{\mathrm{g}}$, where κ^{g} is defined as the largest vote from MSs in S^{g}. The choice $\kappa = \kappa^{\mathrm{g}}$ is a straightforward one because all users in the subscriber group should have a good service under the femtocell. The simulation results are shown in Fig. 7.

In Fig. 7(a), we observe that $\kappa = 1$ is not a good choice in CSG and Hybrid modes. The system throughput in these two modes when $\kappa = 1$ is significantly lower than the one in OSG mode. Additionally, the system throughput is higher when $\kappa = \kappa^{\mathrm{g}}$ compared to the one with $\kappa = 1$ in all modes. The performance degradation results from the reserved resource scheme in SG-FEVER. In this scenario, it is possible that there is still unallocated backhaul data rate in the femtocell when κ is too small. We observed that when $\kappa = \kappa^{\mathrm{g}}$, both OSG and Hybrid modes perform as well as the OSG mode with $\kappa = 1$ when there exist nonsubscriber group MSs.

Although both OSG and Hybrid modes perform well when $\kappa = \kappa^{\mathrm{g}}$ in terms of total system throughput, we have different conclusions from Fig. 7(b). When there are more nonsubscriber group MSs in the overlay system, the average subscriber group throughput decreases to 3.112 and 2.778 Mb/s when $\kappa = 1$ and $\kappa = \kappa^{\mathrm{g}}$ in OSG mode. In contrast, when the SG-FEVER mechanism is in Hybrid mode with $\kappa = \kappa^{\mathrm{g}}$, all subscriber group MSs derive 4 Mb/s downlink data rates, which is their predetermined required throughput. According to the results, Hybrid mode in femtocell system is beneficial to the system and the subscriber group users.

VIII. Conclusion

We proposed a femtocell cell-breathing control framework for determining the optimal coverage of the femtocell and allocating limited femtocell backhaul data rate to MSs fairly and efficiently. The FEVER mechanism, a novel Virtual Election-based mechanism to collect all MSs' QoS information, was proposed. The FEVER mechanism was shown to be truthful, and we proved that through different choices of selected vote order, the balance between system throughput and allocation fairness among MSs can be maintained. We also demonstrated the implementation of the FEVER mechanism in different subscriber group modes by proposing the SG-FEVER mechanism. The LTE-based realistic simulation results not only verify the performance enhancement under the FEVER mechanism, but also show the benefits of Hybrid mode to the overlay system.

APPENDIX

Proof of Theorem 1: First, we prove that the necessary and sufficient condition of M_i to join S_f is $\Gamma_{i,\mathrm{f}}(p) \geq \gamma_{i,\mathrm{f}}$. Given an allocation rule $A(\cdot)$ satisfying Assumption 1 and a femtocell downlink power p, we apply the water-filling algorithm and derive the following allocation:

$$\gamma_{i,\mathrm{f}} = \min\{\Gamma_{i,\mathrm{f}}(p), \gamma_\mathrm{f}(p)\}. \tag{11}$$

We denote the MSs served by the femtocell under the downlink power p by $S_\mathrm{f}(p)$. Then, we denote $S_\mathrm{f}^u(p) = \{M_i | \Gamma_{i,\mathrm{f}}(p) < \gamma_\mathrm{f}(p)\}$ and $S_\mathrm{f}^c(p) = S_\mathrm{f}(p) \setminus S_\mathrm{f}^u(p)$. Thus

$$\sum_{M_i \in S_\mathrm{f}^u(p)} \Gamma_{i,\mathrm{f}}(p) + |S_\mathrm{f}^c(p)|\gamma_\mathrm{f}(p) = \min\{C_\mathrm{f}, \sum \Gamma_{i,\mathrm{f}}(p)\}. \tag{12}$$

Equations (11) and (12) define a unique $r_\mathrm{f}(p)$. In addition, we have $|S_\mathrm{f}|\gamma_\mathrm{f}(p) \geq \sum_{M_i \in S_\mathrm{f}^u(p)} \Gamma_{i,\mathrm{f}}(p) + |S_\mathrm{f}^c(p)|\gamma_\mathrm{f}(p)$. Thus

$$\gamma_\mathrm{f}(p) \begin{cases} \frac{C_\mathrm{f}}{|S_\mathrm{f}|} \geq \frac{C_\mathrm{f}}{|S|} = \frac{C_\mathrm{f}}{N}, & \text{if } \sum \Gamma_{i,\mathrm{f}}(p) \geq C_\mathrm{f} \\ \max_{M_i \in S_\mathrm{f}} \Gamma_{i,\mathrm{f}}(p), & \text{otherwise.} \end{cases} \tag{13}$$

Thus, if M_i chooses to join S_j, its data rate $\gamma_{i,\mathrm{f}}$ satisfies $\Gamma_{i,\mathrm{f}}(p) \geq \gamma_{i,\mathrm{f}} \geq \min\{\Gamma_{i,\mathrm{f}}(p), \frac{C_\mathrm{f}}{N}\} \geq \min\{\Gamma_{i,\mathrm{f}}(p), \gamma_{i,\mathrm{m}}\}$. In addition, we have $\forall M_i \in S$, $\frac{C_\mathrm{f}}{N} \geq \gamma_{i,\mathrm{m}}$. Hence, M_i's best response function is (4) in Theorem 1.

Proof of Theorem 2: We denote $p_i^b = \Gamma_{i,\mathrm{f}}^{-1}(\gamma_{i,\mathrm{m}}) = P_\mathrm{m}\frac{L_{1,\mathrm{m}}}{L_{1,\mathrm{f}}}$ as M_i's boundary power. Without losing generality, given an MS set S, we assume $\frac{L_{1,\mathrm{m}}}{L_{1,\mathrm{f}}} \leq \frac{L_{2,\mathrm{m}}}{L_{2,\mathrm{f}}} \leq \cdots \leq \frac{L_{N,\mathrm{m}}}{L_{N,\mathrm{f}}}$. According to Theorem 1, $p_1^b \leq p_2^b \leq \cdots \leq p_N^b$. Now we discuss the relation among $\gamma_{i,\mathrm{f}}$, p and each MS's peak. We first denote $\Gamma_\mathrm{f}(p) = \sum_{p_i^b \leq p} \Gamma_{i,\mathrm{f}}(p)$. Since $\Gamma(\cdot)$ is an increasing function, $\Gamma_\mathrm{f}(p)$ is an increasing function too. Then, we denote P^F by

$$P^\mathrm{F} = \begin{cases} \Gamma_\mathrm{f}^{-1}(C_\mathrm{f}), & \text{if } \Gamma_\mathrm{f}^{-1}(C_\mathrm{f}) \text{ exists} \\ p_j^{b-}, & \text{otherwise} \end{cases}$$

where $C_\mathrm{f} - \gamma_{j,\mathrm{m}} < \Gamma_\mathrm{f}(p_j^{b-}) < C_\mathrm{f}$. The second case occurs when M_j's joining immediately uses all the unallocated capacity and thus $\Gamma_\mathrm{f}(p_j^{b-}) < C_\mathrm{f}$ and $\Gamma_\mathrm{f}(p_j^b) > C_\mathrm{f}$. Then, we check the following two cases to show that $\gamma_\mathrm{f}(p)$ is increasing when $p < P^\mathrm{F}$ and decreasing when $p > P^\mathrm{F}$:

Recalling (11) and (12), we know $\gamma_{i,\mathrm{f}} = \Gamma_{i,\mathrm{f}}(p)$ $\forall p_i^b \leq p$. Because $\Gamma_{i,\mathrm{f}}(p)$ is an increasing function, $\forall p_i^b \leq p, \gamma_{i,\mathrm{f}}$ is also increasing, and so is $\gamma_\mathrm{f}(p) = \max\{\Gamma_{i,\mathrm{f}}(p)\}$.

Case 2: $p > P^\mathrm{F}$: In this case, we would like to show that $\gamma_\mathrm{f}(p)$ is strictly decreasing with p. We discuss two cases.

Case 2.A: $p_j^b < p < p' < p_{j+1}^b$: Since $p' < p_{j+1}^b$, M_{j+1} chooses not to join S_f'. Thus, $S_\mathrm{f}' = S_\mathrm{f} = \{M_i | i \leq j\}$. According to (12), we have

$$|S_\mathrm{f}^c(p)|\gamma_\mathrm{f}(p') + \sum_{M_i \in S_\mathrm{f}^u(p')} \Gamma_{i,\mathrm{f}}(p) = |S_\mathrm{f}^c(p')|\gamma_\mathrm{f}(p) + \sum_{M_i \in S_\mathrm{f}^u(p')} \Gamma_{i,\mathrm{f}}(p'). \tag{14}$$

We make an assumption that $\gamma_\mathrm{f}(p) \leq \gamma_\mathrm{f}(p')$. Since $p' > p$, $\Gamma_{i,\mathrm{f}}(p') > \Gamma_{i,\mathrm{f}}(p)$ $\forall M_i \in S_\mathrm{f}$. We denote $\Delta S_\mathrm{f}^u = S_\mathrm{f}^u(p) \setminus S_\mathrm{f}^u(p')$. Due to (11), $S_\mathrm{f}^u(p) \subset S_\mathrm{f}^u(p')$. If $\Delta S_\mathrm{f}^u = \emptyset$, $S_\mathrm{f}^c(p') = S_\mathrm{f}^c(p)$ and $S_\mathrm{f}^u(p') = S_\mathrm{f}^u(p)$. We check the left and right parts of (14) term by term and find out the right part of (14) is strictly larger than its left part, which reaches a contradiction. Thus, ΔS_f^u is nonempty. For each $M_i \in \Delta S_\mathrm{f}^u$, we find out that $\Gamma_{i,\mathrm{f}}(p') > \Gamma_{i,\mathrm{f}}(p) > \gamma_\mathrm{f}(p)$. Thus, the right part of (14) is still strictly larger than its left part. Hence, according to the proof of contradiction, our assumption that $\gamma_\mathrm{f}(p) \leq \gamma_\mathrm{f}(p')$ is wrong. Thus, we have $\gamma_\mathrm{f}(p) > \gamma_\mathrm{f}(p')$.

Case 2.B: $p_j^b < p < p_{j+1}^b < p_k^b < p' < p_{k+1}^b$: Since $p_k^b < p' < p_{k+1}^b$, $S_\mathrm{f}' = S_\mathrm{f} \cup \{M_j + 1, M_j + 2, \ldots, M_k\} = S_\mathrm{f} \cup \Delta S_\mathrm{f}$. From (12)

$$C_\mathrm{f} = |S_\mathrm{f}^{c'}(p')|\gamma_\mathrm{f}(p') + \sum_{M_i \in S_\mathrm{f}^{u'}(p')} \Gamma_{i,\mathrm{f}}(p') + |\Delta S_\mathrm{f}^{c'}(p')|\gamma_\mathrm{f}(p') + \sum_{M_i \in \Delta S_\mathrm{f}^{u'}(p')} \Gamma_{i,\mathrm{f}}(p') \tag{15}$$

where $S_\mathrm{f}^{h'}(p') = S_\mathrm{f}^h(p') \setminus \delta S_\mathrm{f}$, $\delta S_\mathrm{f}^{h'}(p') = S_\mathrm{f}^h(p') \cap \delta S_\mathrm{f}$ and $h = \{c, u\}$. We still make an assumption that $\gamma_\mathrm{f}(p) \leq \gamma_\mathrm{f}(p')$. We observe that in (15), the terms with $S_\mathrm{f}^{c'}(p')$ and $S_\mathrm{f}^{u'}(p')$ are just the right part of (14) in Case 2.A, which we have proved strictly larger than the left part. In addition, the third and four terms in the right part of (15) are strictly positive. Thus, we conclude the right part of (15) is strictly larger than its left part. Hence, according to the proof of contradiction, our assumption that $\gamma_\mathrm{f}(p) \leq \gamma_\mathrm{f}(p')$ is wrong. Thus, we have $\gamma_\mathrm{f}(p) > \gamma_\mathrm{f}(p')$.

Finally, we show that each M_i has its peak value p_i^*. According to (11), $\Gamma(\cdot)$ is increasing with p, and $\gamma_\mathrm{f}(p)$ is decreasing with p. Thus, M_i has a unique peak value p_i^* that satisfies $\Gamma_{i,\mathrm{f}}(p_i^*) = (\gamma_\mathrm{f}(p_i^*))$. In addition, $\forall M_i \in S, p_i^* \geq P^\mathrm{F}$ since $\gamma_{i,\mathrm{f}}(p)$ is increasing when $p < P^\mathrm{F}$.

Proof of Theorem 7: Here, we prove this theorem by contradiction. We denote the utilities of MSs under the FEVER mechanism by $\{u_i\}$ and the MSs served by the femtocell by S_f. Then, we assume there exist other utilities of MSs $\{u_i'\}$ that

$$u_k' > u_k \text{ for some } M_k \in S \text{ and } \forall u_i \leq u_k,\ u_i' \geq u_i. \tag{16}$$

We denote the MS/backhaul data rate allocation under $\{u_i'\}$ as S_f' and $\{\gamma_{i,\mathrm{f}}' | M_i \in S_\mathrm{f}'\}$. Then, $\{u_i'\}$ can be denoted as

$$u_i' = \begin{cases} \gamma_{i,\mathrm{f}}', & \text{if } M_i \in S_\mathrm{f}' \\ \Gamma_{i,\mathrm{m}}, & \text{otherwise.} \end{cases}$$

Notice that $S_\mathrm{f}' \neq S_\mathrm{f}$ must hold. Otherwise, the expected throughput of all MSs will be equal under both S_f and S_f' and we have a contradiction. Now we examine the candidates of M_k and show the contradictions in every cases.

Case 1: $M_k \in S \setminus S_\mathrm{f}$: We recall (4) in Theorem 1. Given M_k in $S \setminus S_\mathrm{f} = S_\mathrm{m}$, we have $u_k = \Gamma_{k,\mathrm{m}} > \Gamma_{k,\mathrm{f}}(p) \geq \gamma_{k,\mathrm{f}}'$. Thus, if $M_k \in S_\mathrm{f}'$, $u_k' = \gamma_{k,\mathrm{f}}' < \Gamma_{i,\mathrm{m}} = u_k$. However, if $M_k \notin S_\mathrm{f}'$, $u_k' = \Gamma_{k,\mathrm{f}} = u_k$. Both possibilities lead to the contradiction.

Case 2: $M_k \in S_\mathrm{f} \cap (S \setminus S_\mathrm{f}')$: Recalling (4) in Theorem 1 and given $M_k \in S_\mathrm{f}$ and $M_k \in S \setminus S_\mathrm{f}'$, we have $u_k > \Gamma_{k,\mathrm{m}} = u_k'$, which leads to the contradiction.

Case 3: $M_k \in S_\mathrm{f} \cap S_\mathrm{f}'$: We first discuss the case that $S_\mathrm{f} \neq S_\mathrm{f}'$. Given $M_k \in S_\mathrm{f}' \cap S_\mathrm{f}$, we have $u_k' = \gamma_{i,\mathrm{f}}'$ since $M_k \in S_\mathrm{f}'$. In addition, we have $u_k' > u_k = \gamma_{i,\mathrm{f}}(p)$. However, recalling (11) in the proof of Theorem 1, since $u_k' > u_k$ and the maximum utility of M_k is $\Gamma_{i,\mathrm{f}}(p)$, $\Gamma_{i,\mathrm{f}}(p) > \gamma_\mathrm{f}(p)$ and $u_k = \gamma_\mathrm{f}(p)$. Thus, we have $\forall M_i \in S_\mathrm{f}$, $u_k = \gamma_\mathrm{f}(p) \geq u_i$. Hence, if there exists $M_i \in S_\mathrm{f} \cap (S \setminus S_\mathrm{f}')$, according to (4) its utility will be $u_i' = \Gamma_{i,\mathrm{m}} < \gamma_{i,\mathrm{f}} = u_i$. In addition, if there exists $M_i \in (S \setminus S_\mathrm{f}) \cap (S_\mathrm{f}')$, according to (4) its utility will be $u_i' \leq \Gamma_{i,\mathrm{f}} < \Gamma_{i,\mathrm{m}} = u_i$. Both cases violate (16) and lead to the

contradiction. Since all cases have been discussed, according to the proof of contradictions, there exists no $\{u_i'\}$ satisfying (16) with $S_{\mathrm{f}}' \neq S_{\mathrm{f}}$. This completes the proof.

REFERENCES

[1] H. Claussen, L. T. W. Ho, and L. G. Samuel, "An overview of the femtocell concept," *Bell Labs Tech. J.*, vol. 13, no. 1, pp. 221–245, 2008.

[2] V. Chandrasekhar, J. Andrews, and A. Gatherer, "Femtocell networks: a survey," *IEEE Commun. Mag.*, vol. 46, no. 9, pp. 59–67, Sep. 2008.

[3] *Modulation and coding set design for IEEE 802.16m system*, IEEE C802.16m-09/0216, Jan. 2009.

[4] Alcatel-Lucent, "DL E-UTRA performance checkpoint," 3GPP TSG-RAN1, Tech. Rep. R1-071967, 2007.

[5] A. Golaup, M. Mustapha, and L. B. Patanapongpibul, "Femtocell access control strategy in UMTS and LTE," *IEEE Commun. Mag.*, vol. 47, no. 9, pp. 117–123, Sep. 2009.

[6] R. Farquharson, *Theory of Voting*. Oxford, U.K.: Blackwell, 1969.

[7] P. Xu, X. Xu, S. Tang, and M. Li, "Truthful online spectrum allocation and auction in multi-channel wireless networks," in *Proc. IEEE INFOCOM*, Shanghai, China, Apr. 2011, pp. 26–30.

[8] H. Zhang *et al.*, "A framework for truthful online auctions in cloud computing with heterogeneous user demands," in *Proc. IEEE INFOCOM*, Apr. 2013, pp. 1510–1518.

[9] ITU, "ITU-R Guidelines for evaluation of radio interface technologies for IMT-Advanced," Tech. Rep. ITU-R M. 2135, 2008.

[10] C. Mehlführer, M. Wrulich, J. C. Ikuno, D. Bosanska, and M. Rupp, "Simulating the long term evolution physical layer," in *Proc. 17th EUSIPCO*, Glasgow, Scotland, Aug. 2009, pp. 1471–1478.

[11] V. Veeravalli and A. Sendonaris, "The coverage-capacity tradeoff in cellular CDMA systems," *IEEE Trans. Veh. Technol.*, vol. 48, no. 5, pp. 1443–1450, Sep. 1999.

[12] A. Jalali, "On cell breathing in CDMA networks," in *Proc. IEEE ICC*, Jun. 1998, vol. 2, pp. 985–988.

[13] S.-T. Yang and A. Ephremides, "Resolving the CDMA cell breathing effect and near-far unfair access problem by bandwidth-space partitioning," in *Proc. IEEE VTC*, May 2001, vol. 2, pp. 1037–1041.

[14] P. Bahl *et al.*, "Cell breathing in wireless LANs: Algorithms and evaluation," *IEEE Trans. Mobile Comput.*, vol. 6, no. 2, pp. 164–178, Feb. 2007.

[15] Y. Bejerano and S.-J. Han, "Cell breathing techniques for load balancing in wireless LANs," *IEEE Trans. Mobile Comput.*, vol. 8, no. 6, pp. 735–749, Jun. 2009.

[16] S.-p Yeh, S. Talwar, S.-c Lee, and H. Kim, "WiMAX femtocells: a perspective on network architecture, capacity, and coverage," *IEEE Commun. Mag.*, vol. 46, no. 10, pp. 58–65, Oct. 2008.

[17] H. A. Mahmoud and I. Guvenc, "A comparative study of different deployment modes for femtocell networks," in *Proc. IEEE PIMRC*, Sep. 2009, pp. 1–5.

[18] D. Choi, P. Monajemi, K. Shinjae, and J. Villasenor, "Dealing with loud neighbors: The benefits and tradeoffs of adaptive femtocell access," in *Proc. IEEE GLOBECOM*, Nov. 2008, pp. 1–5.

[19] A. Valcarce, D. Lopez-Perez, G. D. La Roche, and Z. Jie, "Limited access to OFDMA femtocells," in *Proc. IEEE PIMRC*, Sep. 2009, pp. 1–5.

[20] G. d. l. Roche, A. Valcarce, D. Lopez-Perez, and Z. Jie, "Access control mechanisms for femtocells," *IEEE Commun. Mag.*, vol. 48, no. 1, pp. 33–39, Jan. 2010.

[21] T. Akbudak and A. Czylwik, "Distributed power control and scheduling for decentralized OFDMA networks," in *Proc. IEEE WSA*, Feb. 2010, pp. 59–65.

[22] X. Li, L. Qian, and D. Kataria, "Downlink power control in co-channel macrocell femtocell overlay," in *Proc. 43rd CISS*, 18–20, 2009, pp. 383–388.

[23] E. Jorswieck and R. Mochaourab, "Power control game in protected and shared bands: Manipulability of Nash equilibrium," in *Proc. GameNets*, May 2009, pp. 428–437.

[24] J. L. Boudec, "Rate adaptation, congestion control and fairness: A tutorial," 2005.

[25] N. Nisan, T. Roughgarden, and V. V. Vazirani, *Algorithmic Game Theory*. Cambridge, U.K.: Cambridge Univ. Press, 2007.

[26] S. Ching, "Strategy-proofness and median voters," *Int. J. Game Theory*, vol. 26, no. 4, pp. 473–490, 1997.

[27] R. Jain, A. Durresi, and G. Babic, "Throughput fairness index: an explanation," in *Proc. ATM Forum*, 1999, vol. 45, Contribution 99.

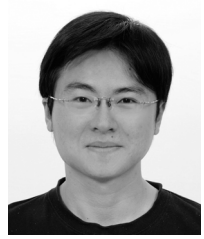

Chih-Yu Wang received the B.S. and Ph.D. degrees in electrical engineering and communication engineering from National Taiwan University (NTU), Taipei, Taiwan, in 2007 and 2013, respectively.

He was a visiting student with the University of Maryland, College Park, MD, USA, in 2011. He is currently an Assistant Research Fellow with the Research Center for Information Technology Innovation, Academia Sinica, Taipei, Taiwan. His research interests include game theory, wireless communications, social networks, and data science.

Chun-Han Ko received the B.S. and M.S. degrees in electrical engineering and communication engineering from National Taiwan University (NTU), Taipei, Taiwan, in 2007 and 2009, respectively, and is currently pursuing the Ph.D. degree in communication engineering at NTU.

His research interests include incentive mechanism design and game-theoretic optimization for communication networks.

Hung-Yu Wei received the B.S. degree from National Taiwan University (NTU), Taipei, Taiwan, in 1999, and the M.S. and Ph.D. degrees from Columbia University, New York, NY, USA, in 2001 and 2005, respectively, all in electrical engineering.

He is currently an Associate Professor with the Department of Electrical Engineering and Graduate Institute of Communication Engineering, NTU. He was a consulting member of the Acts and Regulation Committee of the National Communications Commission during 2008–2009. He actively participates in wireless network standardization activities. His research interests include wireless networking and game-theoretic models for networking.

Dr. Wei was the recipient of the Recruiting Outstanding Young Scholar Award from the Foundation for the Advancement of Outstanding Scholarship in 2006, the NTU Excellent Teaching Award in 2008, and the K. T. Li Young Researcher Award from ACM Taipei/Taiwan in 2012. He was awarded the Research Project for Excellent Young Scholars from Ministry of Science and Technology in 2014.

Athanasios V. Vasilakos (M'00–SM'11) received the Ph.D. degree in computer engineering from the University of Patras, Patras, Greece, in 1988.

He is currently a Professor with Kuwait University, Safat, Kuwait.

Prof. Vasilakos served or is serving as an Editor or/and Guest Editor for many technical journals, such as the IEEE TRANSACTIONS ON NETWORK AND SERVICE MANAGEMENT, IEEE TRANSACTIONS ON CLOUD COMPUTING, IEEE TRANSACTIONS ON INFORMATION FORENSICS AND SECURITY, IEEE TRANSACTIONS ON NANOBIOSCIENCE, IEEE TRANSACTIONS ON CYBERNETICS, IEEE TRANSACTIONS ON INFORMATION TECHNOLOGY IN BIOMEDICINE, *ACM Transactions on Autonomous and Adaptive Systems*, and IEEE JOURNAL ON SELECTED AREAS IN COMMUNICATIONS. He is also General Chair of the European Alliances for Innovation.